DOES BLOCKING OF FIBROBLAST GROWTH FACTOR-1 AND ITS RECEPTORS AFFECT MOUSE PERIPHERAL NERVE MYELINATION?

by

Büşra Şimşek

B.S., Molecular Biology and Genetics, Istanbul Technical University, 2012

Submitted to the Institute for Graduate Studies in
Science and Engineering in partial fulfilment of
the requirements for the degrees of
Master of Science

Graduate Program in Molecular Biology and Genetics

Boğaziçi University

2015

To my family…

ACKNOWLEDGEMENTS

I would like to express my deepest appreciation to my thesis supervisor Prof. Esra Battaloğlu for great support throughout the project. Without her incredible patience and valuable guidance, this work would not have been possible. Being her student is a big chance for me.

I would like to thank Prof. Kuyaş Buğra for giving me guiding advices whenever I consulted her during the project and also accepting to be a member of my thesis committee.

I would like to express my special gratitude to Duygu Dağlıkoca who was a former member of our laboratory. She was always available for my questions and shared generously her valuable time and knowledge with me.

I specially would like to thank my current laboratory member Burçak Özeş for her support, help and precious friendship during my three years in the laboratory. I am also grateful to Ayşe Candayan and Oğuz Arı. I appreciate Neslihan Zöhrap, Aslı Uğurlu, Burcu Ersoy and Mahmutcan Hız for their helps in particular methods in this research. I would like to thank again Burcu Ersoy for her moral support while writing this thesis.

I appreciate helps of Arzu Temizyürek. Apart from animal handling and taking good care of my mice at the Center for Life Sciences and Technologies, she also assisted me during the sciatic nerve injections.

I would like to express my deepest gratitude and thanks to each member of my family for their support and endless love throughout my life.

Finally, I would like to thank The Scientific and Technological Research Council of Turkey 2210-National Scholarship Programme for granting during first two years of my study. I also appreciate Scientific Research Project (BAP) for financially supporting me and this project (14B01P7).

ABSTRACT

DOES BLOCKING OF FIBROBLAST GROWTH FACTOR-1 AND ITS RECEPTORS AFFECT MOUSE PERIPHERAL NERVE MYELINATION?

Bi-directional communication between axon and Schwann cell is vital to the peripheral nervous system (PNS) myelination process. Disruption of this highly regulated communication is the main underlying reason of peripheral neuropathies. Understanding the molecular mechanism of this interaction is important to unravel the pathology of these diseases. Previous studies performed in our laboratory demonstrated that FGF1 is localized to axons, whereas FGF receptors are localized to Schwann cells, similar to that of NRG1 that is the most well-known protein acting in this interaction. Moreover, *in vitro* studies have shown that FGF1 may have a possible role during PNS myelination. Thus, in this study, we aimed to further investigate the possible role of FGF1 and its receptors (FGFR1-3) during PNS myelination process through *in vivo* experiments. For this purpose, we used mouse sciatic nerve as an *in vivo* model of PNS and used PNS remyelination procedure in which lysolecithin-induced demyelination promotes a remyelination period that mimick developmental myelination. Initially, we determined the time points for demyelination-remyelination processes through immunohistochemistry and western blotting. Secondly, we blocked FGF1 and its receptors one by one during remyelination period and investigated their effect on remyelination *via* western blot analysis. The results of this study further demonstrated that FGF1 has a possible role during PNS myelination process, but probably in an intracrine manner. Together with the studies previously performed in our laboratory, this study provides evidence for the involvement of FGF1 in PNS myelination process that has not been demonstrated previously in the literature.

ÖZET

FİBROBLAST BÜYÜME FAKTÖRÜ-1 VE RESEPTÖRLERİNİN BLOKLANMASI FARE PERİFERAL SİNİR SİSTEMİ MİYELİNİZASYONUNU ETKİLER Mİ?

Akson ve Schwann hücre arasındaki çift yönlü iletişim periferal sinir sistemi (PSS) miyelinizasyonu açısından hayati öneme sahiptir. Son derece regüle olan bu iletişimde meydana gelen sorunlar periferal nöropatilerin altında yatan ana sebeplerden biridir. Bu iletişimin moleküler mekanizmasının anlaşılması, periferal nöropatilerin patogenezinin aydınlatılması açısından önemlidir. Laboratuvarımızda daha önceki yıllarda yapılan çalışmalar FGF1'in, akson-Schwann hücre etkileşimde rol aldığı bilinen NRG1'e benzer şekilde, aksonlarda, reseptörlerinin ise Schwann hücrelerinde lokalize olduğunu göstermiştir. Ayrıca, yapılan in *vitro* çalışmalar FGF1'in PSS miyelinizasyonunda olası bir role sahip olabileceğini ortaya koymuştur. Bu nedenle, bu çalışmada FGF1 ve reseptörlerinin PSS miyelinizasyonundaki olası rollerinin in *vivo* deneyler aracılığıyla daha ayrıntılı araştırılması hedeflenmiştir. Bu amaçla fare siyatik siniri PSS in *vivo* modeli olarak kullanılmıştır. Ayrıca gelişim sürecindeki miyelinizasyonu temel olarak benzer olması dolayısıyla PSS remyelinizasyon prosedürü kullanılmıştır. Bu prosedürde lizolesitin ile oluşturulan demiyelinizasyon remiyelinizasyonu sürecini tetikler. Çalışmada ilk olarak, immünohistokimya ve western blotlama teknikleri kullanılarak demiyelinizasyon-remiyelinizasyon süreçlerinin başlangıç ve bitiş zamanları belirlenmiştir. İkinci olarak, FGF1 ve reseptörleri remiyelinizasyon sürecinde ayrı ayrı bloklanıp, remiyelinizasyon sürecine etkileri western blotlama tekniği aracılığıyla incelenmiştir. Bu çalışma, FGF1'in PSS miyelinizasyon sürecinde etkili olabileceğini bir kez daha göstermiştir, fakat tahmin edildiği gibi reseptörler aracılığıyla değil reseptörlerden bağımsız bir şekilde. Laboratuvarımızda önceki yıllarda yapılan çalışmalarla birlikte bu çalışma, FGF1'in PSS miyelinizasyon sürecinde bir role sahip olabileceğini literatürde ilk defa ortaya koymuştur.

TABLE OF CONTENTS

ACKNOWLEDGEMENTS iv

ABSTRACT v

ÖZET vi

LIST OF FIGURES xi

LIST OF TABLES xiv

LIST OF SYMBOLS xv

LIST OF ACRONYMS/ABBREVIATIONS xvi

1. INTRODUCTION 1

1.1. The Myelin Sheath in Peripheral Nervous System 1

1.1.1. Myelin Proteins 2

1.2. Schwann Cell Myelination 3

1.2.1. Mechanism of Schwann Cell Myelination 5

1.2.2. Axon-Schwann Cell Interactions 7

1.2.3. Transcriptional Regulation of Myelination 9

1.3. Schwann Cell Remyelination 10

1.3.1. Molecular Mechanism of Schwann Cell Remyelination 11

1.4. Lysolecithin-induced Demyelination 12

1.5. Fibroblast Growth Factors 13

1.5.1. FGF1 (Acidic FGF) 14

1.6. Fibroblast Growth Factor Receptors 14

1.7. Signaling Through FGFRs 16

1.8. Fibroblast Growth Factors and Receptors in the Nervous System 17

1.8.1. Fibroblast Growth Factors and Receptors in Myelination 19

1.9. Previous Studies Performed in Our Laboratory 19

2. AIM OF THE STUDY 21

3. MATERIALS 23

3.1. Mice Strain 23

3.2. Chemicals 23

3.3. Buffers and Solutions 24

3.4. Antibodies 27

3.5. Disposable Materials 30

3.6. Equipment 30

4. METHODS 32

4.1. Sciatic Nerve Injection 32

4.2. Lysolecithin Induced Demyelination 32

4.3. Antibody Mediated FGF1 Blocking 33

4.4. Antibody Mediated FGFR1, FGFR2 and FGFR3 Blocking 33

4.5. Preparation of Sciatic Nerve Tissue Homogenate 34

4.6. Immunoprecipitation 34

4.7. Western Blot Analysis 35

4.8. Tissue Processing and Imunohistochemistry 36

4.9. Statistical Analysis 36

5. RESULTS 38

5.1. Injection of 2% LPC Solution Induces Demyelination in Mouse Sciatic Nerve ...38

5.2. Remyelination Starts Approximately 7 Days After LPC Injection 42

5.3. Schwann Cell Number is Increased During Remyelination 44

5.4. FGF1 Level is Upregulated during Remyelination, While FGF2 is 50

5.5. Blocking of FGF1 Cause Reduction in Remyelination 51

5.5.1. 20 µg/ml of FGF1 Neutralizing Antibody (Ab9588) Efficiently Blocks FGF1 *in vivo* 51

5.5.2. Blocking of FGF1 During Remyelination Causes a Decrease in MBP and MAG Expression 53

5.6. Blocking of FGFR1, FGFR2 and FGFR3 Has No Significant Effect on Remyelination 55

5.6.1. FGFR1 Blocking 55

5.6.1.1. Signaling Pathway Activated by FGFR1 During Remyelination 57

5.6.2. FGFR2 Blocking 59

5.6.3. FGFR3 Blocking 61

5.7. FGF1 Blocking Did Not Affect Phosphorylation of FGFR1, FGFR2 and FGFR2 62

6. DISCUSSION 64

7. CONCLUSION 71

REFERENCES 72

LIST OF FIGURES

Figure 1.1. Neural crest cells and neurulation. 4

Figure 1.2. Schwann cell lineage. 5

Figure 1.3. Fetal nerve fibers. 6

Figure 1.4. Radial sorting of an individual axon and myelination. 6

Figure 1.5. Myelin formation by the wrapping of the inner lip around axon. 7

Figure 1.6. Myelination in mouse mutant lacking NRG1 (-/-), in heterozygous NRG1 (-/+) mice, and in transgenic mice overexpressing NRG1. 8

Figure 1.7. Nectin-like protein interactions in internodes and Schmidt-Lanterman incisures..... 9

Figure 1.8. Schematic representation of demyelination and remyelination in PNS. 11

Figure 1.9. Three-dimentional structure of FGF2 protein showing receptor (red) and heparin binding sites (blue). 14

Figure 1.10. FGFR structure and dimerization after binding to FGFs and proteoglycan. 15

Figure 1.11. FGFR isoforms created through alternative splicing of the Ig-like III encoding region. 16

Figure 1.12. The FGF-FGFR signaling pathway. 17

Figure 5.1. Immunolabelling of adult mouse sciatic nerve for NF and MBP. 39

Figure 5.2. Immunolabelling of adult mouse sciatic nerve injected with 1% of LPC solution for MBP and NF. 40

Figure 5.3. Immunolabelling of adult mouse sciatic nerve for MBP that has been injected with 2% of lysolecithin. 41

Figure 5.4. Western blotting of MBP after 1, 7, 15 and 21 days from LPC injection. ..42

Figure 5.5. Western blotting of MAG after 1, 7, 15 and 21 days from LPC injection. .43

Figure 5.6. Immunolabelling of adult mouse sciatic nerve for MBP and NF dissected 7 days after lysolecithin injection. 45

Figure 5.7. Immunolabelling of adult mouse sciatic nerve for MBP dissected 14 days after lysolecithin injection. 47

Figure 5.8. Immunolabelling of adult mouse sciatic nerve dissected 28 day after lysolecithin injection for MBP. 48

Figure 5.9. Number of nuclei in immunolabelling of adult mouse sciatic nerve dissected 7, 14 and 28 days after lysolecithin injection. 49

Figure 5.10. Western blotting of FGF1 and FGF2 after 1, 7, 15 and 21 day from LPC injection. 50

Figure 5.11. Western blotting of p-FGFR after 10 and 20 µg/ml anti-FGF1 neutralizing antibody injection. 52

Figure 5.12. Western blotting of p-FGFR 20 µg/ml anti-FGF1 neutralizing antibody injection. 53

Figure 5.13. Western blotting of MAG after two repetitive injections of anti-FGF1 blocking antibody following demyelination. 54

Figure 5.14. Western blotting of MBP after two times injection of anti-FGF1 blocking antibody following demyelination. 54

Figure 5.15. Western blotting of MBP after two repetitive injections of anti-FGFR1 blocking antibody following demyelination. 56

Figure 5.16. Western blotting of MAG after two repetitive injections of anti-FGFR1 blocking antibody following demyelination. 57

Figure 5.17. Western blotting of p-ERK1, p-AKT and p-PLC gamma 1 after two repetitive injections of anti-FGFR1 blocking antibody. 58

Figure 5.18. Western blotting of MAG after two repetitive injections of anti-FGFR2 neutralizing antibody following demyelination. 60

Figure 5.19. Western blotting of MBP after two repetitive injections of anti-FGFR2 neutralizing antibody following demyelination. 60

Figure 5.20. Western blotting of MAG and MBP after two repetitive injections of anti-FGFR3 neutralizing antibody following demyelination. 61

Figure 5.21. MAG and MBP protein levels relative to actin after two repetitive injections of anti-FGFR3 neutralizing antibody following demyelination. . 62

Figure 5.22. Immunoblotting of immunoprecipitated FGFR1, FGFR2 and FGFR3 for p-FGFR after FGF1 blocking. 63

LIST OF TABLES

Table 3.1. Chemicals used in this study. 23

Table 3.2. Buffers or solutions for western blot analysis. 24

Table 3.3. Buffers or solutions used for tissue processing and immunohistochemistry. 26

Table 3.4. Primary antibodies used for western blot analysis. 27

Table 3.5. List of secondary antibodies used for western blot analysis. 28

Table 3.6. Primary antibodies used for immunohistochemistry. 28

Table 3.7. Secondary antibodies used for immunohistochemistry. 29

Table 3.8. Neutralizing antibodies used in this study. 29

Table 3.9. Isotype control immunoglobulins used in this study. 30

Table 3.10. Disposable materials used in this study. 30

Table 3.11. Laboratory equipment used in this study. 31

LIST OF SYMBOLS

ml	milliliter
mg	milligram
µl	microliter
µg	microgram
V	volt
kDa	kilodalton
mM	millimolar
M	molar

LIST OF ACRONYMS/ABBREVIATIONS

AKT	V-akt murine thymoma viralonco gene
APS	Ammonium per sulphate
BCA	Bicinchoninic acid
BL	Basal lamina
BSA	Bovine serum albümin
CMT	Charcot-Marie-Tooth
CNS	Central nervous system
DABCO	1,4-diazabicyclo[2.2.2]octane
DAG	Diacylglycerol
DAPI	4',6-diamidino-2-phenylindole
DNA	Deoxyribonucleic acid
DRG	Dorsal root ganglion
E12/13	Embryonic day 12/13
E15/16	Embryonic day 15/16
EDTA	Ethylenediaminetetraacetic acid
EGR2	Early growth response gene-2
ErbB2/3	v-erb-b2 a*via*n erythroblastic leukemia viral oncogene
ERK 1/2	Extracellular signal-regulated kinase 1/2
ERK	Extracellular signal-regulated kinase
FABP	Fatty acid binding protein
FGF	Fibroblast growth factor
FGF1	Fibroblast growth factor 1
FGF2	Fibroblast growth factor 2
FGFR	Fibroblast growth factor receptor
FGFR1	Fibroblast growth factor 1
FGFR2	Fibroblast growth factor 2
FGFR3	Fibroblast growth factor 3
FGFR4	Fibroblast growth factor 4
FRS2	FGF receptor substrate 2

Grb2	Growth factor receptor-bound protein 2
HCl	Hydrochloric acid
HNPP	Hereditary neuropathy with liability to pressure palsies
HRP	Horseradish peroxidase
IGF-1	Insulin-like growth factor-1
IgG	Immunoglobulin G
Ig-like	Immunoglobulin-like
IP3	Triphosphate 3
JNK	c-Jun N-terminal kinase
Krox-20	Egr2 early growth response 2
LPC	Lysophosphatidycholine
MAG	Myelin asssociated glycoprotein
MAPK	Mitogen activated protein kinase
MBP	Myelin basic protein
MMP-9	Matrix metallopeptidase-9
NaCl	Sodium chloride
Necl1	Nectin-like 1
Necl2	Nectin-like 2
Necl4	Nectin-like 4
NF	Nuclear factor
NRG1	Neurogulin 1
OCT	Optimum cutting temperature
Oct-6	Octamer transcription factor 6
OPC	Oligodendrocyte precursor cell
P0	Myelin protein zero
P10	Postnatal day 10
P7	Postnatal day 7
p-AKT	phospho-AKT
PBS	Phosphate buffered saline
p-ERK	phospho-ERK
PFA	Paraformaldehyde
p-FGFR	phosho-FGFR

PI3K	Phosphatidylinositol 3-kinase
PKB	Protein kinase B
PKC	Protein kinase C
PLCγ	Phosphoinositide phospholipase C gamma
PMP22	Peripheral myelin protein 22
PNS	Peripheral nervous system
p-PLCγ	phospho-PLC gamma
PVDF	Polyvinylidene difluoride
RIPA	Radioimmunoprecipitation assay
rpm	Revolution per minute
SC	Schwann cell
SCPs	Schwann cell precursors
SDS	Sodium dodecyl suphate
SEM	Standart error of mean
SOS	Son of sevenless
Sox-10	SRY (sex determining region Y)-box 10
TBS	Tris buffered saline
TBST	Tris buffered saline with Tween-20
TEMED	N,N,N',N'-tetramethylethylenediamine

1. INTRODUCTION

Schwann cells are the major glial cells that wrap and myelinate axons in the peripheral nervous system (PNS) [1]. There is a constant and dynamic interaction between axons and Schwann cells both during development and adulthood, each one affecting and organizing the development, maintenance and function of the other [2]. This reciprocal interaction between axon and Schwann cell is required for the formation of functional myelinated fibers and any alterations in axon-Schwann cell interaction is known to be responsible for development of peripheral neuropathies [3].

1.1. The Myelin Sheath in Peripheral Nervous System

Myelin sheath is a greatly extended and specialized membrane that insulates axons and enables faster transmission of nerve impulses. In the PNS, the myelin sheath is formed by Schwann cells through extension, biochemical modification and wrapping of its plasma membrane around axons [4]. Each Schwann cell myelinates only one segment of a given axon. To generate an electrically insulating myelin sheath, Schwann cells accumulate large amounts of non-conducting material around segments of the axons and exclude cytosolic material from the structure, forming compact myelin. In myelinated axons, the only region exposed to the extracellular space is the nodes of Ranvier, which are located between two myelinated segments. Access to the entire structure is enabled by Schmidt-Lanterman incisures that are the narrow cytoplasmic channels running spirally through the sheath.

The main role of the myelin sheath is to facilitate the conduction of action potentials along the axon [5]. In unmyelinated axons, the impulse is propagated by local circuits of ion currents which then spread to the adjacent region of membrane in a consecutive manner. In myelinated axons, the local circuit is generated at the nodes of Ranvier that is rich in sodium channels. The circuit cannot flow through the myelin sheath, instead jumps to the next node and this type of impulse propagation is called saltatory conduction. The myelin sheath, through its low capacitance, reduces the energy consumption for the depolarization of the membrane between the nodes and allows an increased speed of local circuit spreading [6].

Lipids account for 70-80% of the myelin dry mass differentiating myelin from other biological membranes with its high lipid-to-protein ratio. Together with particular characteristics of lipids present in the sheath, this relatively high lipid content generates an electrically non-conductive sheath. Cholesterol, galactocerebroside, sulfatides and phosphoglycerides are the major lipids found in the myelin structure. Proteins, on the other hand, constitute 20-30% of the dry mass of PNS myelin. At least 60% of the proteins present in PNS myelin structure are glycosylated, which are myelin protein zero (MPZ), peripheral myelin protein 22 (PMP22) and myelin associated glycoprotein (MAG). Basic proteins are the second most abundant protein group in this membrane including the myelin basic protein (MBP) and the protein P2 [5].

1.1.1. Myelin Proteins

MPZ is the major protein of PNS myelin, comprising more than half of the total protein mass. MPZ is a 30 kDa transmembrane glycoprotein that belongs to the immunoglobulin (IgG) superfamily and consists of three distinct structural domains: a single extracellular Ig-like domain, a hydrophobic transmembrane domain and an intracellular domain [7]. The amino-terminal extracellular domain has a single site for N-linked glycosylation [4, 6]. MPZ functions as a cell adhesion molecule in PNS and enables the very tight compaction of the myelin structure by homophilic interactions. Both intracellular and extracellular domains of MPZ are involved in this interaction and stabilize the major dense lines and intraperiod lines of compact myelin, respectively [7]. MPZ undergoes post-translational modifications, such as glycosylation, acylation and phosphorylation that have important regulatory roles in adhesion. Mutations affecting the phosphorylation of MPZ cause Charcot-Marie-Tooth (CMT) type 1B [8]. Besides, more than 120 different MPZ mutations are known to be causative in CMT and they are distributed throughout the gene [9].

PMP-22 is another glycoprotein that is localized in compact myelin structure of PNS. It is 22 kDa integral membrane protein that comprises less than 5% of the total protein. PMP22 has four hydrophobic transmembrane domains with two extracellular loops. Similar to MPZ, there is a single site on PMP22 molecule for N-linked glycosylation found in its first putative extracellular loop. Unlike MPZ, PMP22 is not only expressed in PNS, but in

many other tissues such as lung, gut, brain and heart [5, 6, 10]. Alterations in PMP22 levels as a result of chromosomal aberrations or mutations in the *PMP22* gene cause inherited peripheral neuropathies, including CMT1A and hereditary neuropathy with liability to pressure palsies (HNPP) [11].

MAG is a transmembrane glycoprotein which represents only 0.1% of PNS myelin proteins. MAG has a molecular weight of 100 kDa and is a member of the immunoglobulin superfamily. In the PNS, it is localized to periaxonal membrane of myelin forming Schwann cells, membranes of Schmidt-Lanterman incisures, paranodal loops, and the external/internal mesaxons. MAG consists of five IgG-like extracellular domains, a transmembrane domain, and a cytosolic domain. It has two isoforms known as: S-MAG and L-MAG. Although both isoforms are expressed in PNS, S-MAG is the predominant form both during development and adulthood. MAG expression starts at early stages of myelination and continues at a relatively high level during the adulthood suggesting that it functions both in early axon-Schwann cell interaction and in the maintenance of myelin and the myelinated axons [12, 13].

MBP is a basic myelin protein that accounts for 5% to 18% of total protein in PNS. It has four isoforms with molecular weight of 21, 18.5, 17 and 14 kDa which are produced by the same gene through alternative splicing. MBP in PNS is thought to contribute to the compaction of cytoplasmic side of myelin together with MPZ [5, 6].

The basic P2 protein is a member of fatty acid binding protein (FABP) family with a molecular weight of 14.8 kDa. Similar to MBP, it is located in the cytoplasmic side of the compact myelin but unlike other myelin proteins, its amount varies considerably in different species. Since it is present in the major dense line of myelin sheaths, it may have a structural role similar to MBP. Furthermore, its lipid binding affinity suggests that it may be involved in the assembly and turn-over of the myelin membrane lipids [5, 6, 14].

1.2. Schwann Cell Myelination

Glial cells are the second most abundant cell types in the nervous system. They allow development of the nervous system by forming a cellular framework and regulate neuronal

survival and differentiation. The most well-known function of the glial cells is to myelinate the axons [15]. Schwann cells that are the major glial cell of the PNS lack the ability to transmit synaptic messages and can undergo cell division indefinitely throughout their survival [16].

The myelinating and nonmyelinating Schwann cells in the peripheral system arise from neural crest cells that emerge at the most dorsal part of the neural tube during the neurulation process (Figure 1.1) [17]. Neural crest cells also give rise to neural cells of the sensory, autonomic and enteric nervous system as well as nonneural cells including melanocytes and smooth muscle cells [1, 17].

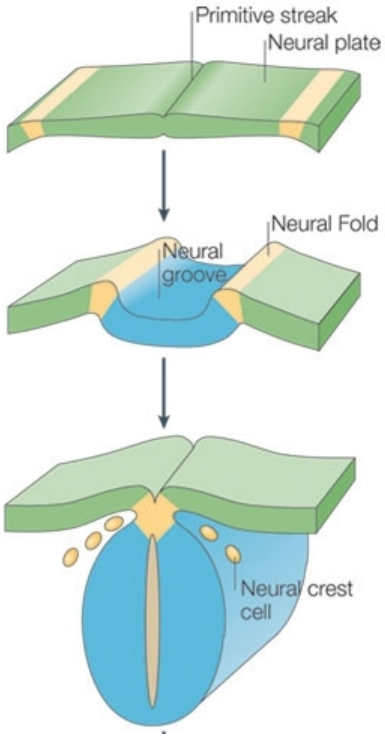

Figure 1.1. Neural crest cells and neurulation. Neural crest cells delaminate from the most dorsal part of the neural tube during neurulation process and migrate in a ventral direction to give rise to Schwann cell precursors [18].

Schwann cell generation is a long process consisting of two embryonic transitional stages. In the first step, the neural crest cells differentiate into Schwann cell precursors (SCPs) through the gliogenesis process that occurs at embryonic day 12/13 (E12/13). These

cells turn into immature Schwann cells at around day E15/16 in the second stage. The postnatal fate of immature Schwann cells is determined by the diameter of the axon with which they associate. Immature Schwann cells that associate with large diameter axons differentiate into myelinating Schwann cells, whereas those that interact with small diameter axons become non-myelinating Schwann cells (Figure 1.2). These processes are regulated by the survival factors, mitogens, and differentiation signals secreted from the axons [18]. Remarkably, both myelinating and nonmyelinating Schwann cells have the ability to dedifferentiate into immature phenotype in response to nerve injury. Thus, they can actively promote functional recovery [19].

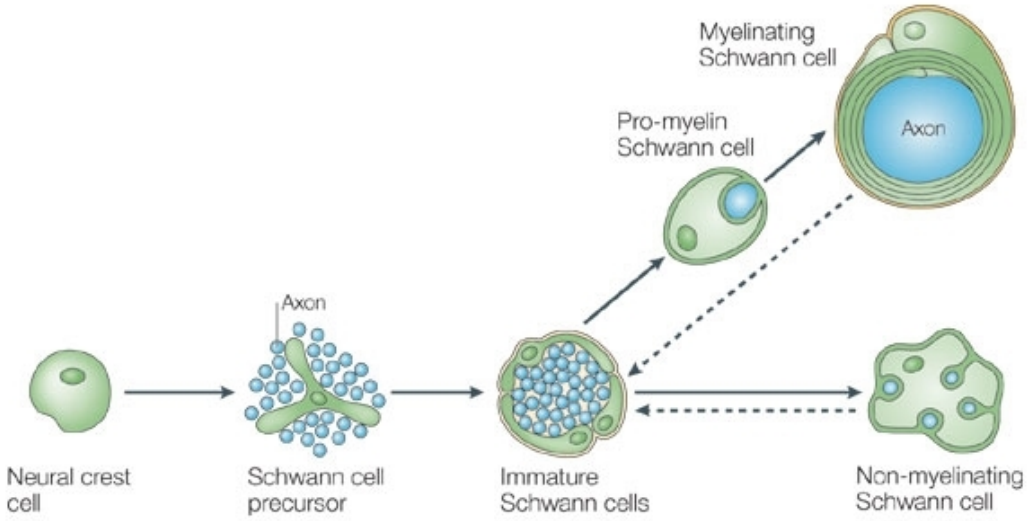

Figure 1.2. Schwann cell lineage. Both myelinating and nonmyelinating Schwann cells are differentiated from immature Schwann cells which originates from neural crest cells [18].

1.2.1. Mechanism of Schwann Cell Myelination

Schwann cell myelination process consists of three stages because of sequential appearance of three different nerve fibers. At the onset of PNS myelination, a single thin layer of Schwann cells envelop a large bundle of naked axons comprising fetal nerve fibers (Figure 1.3). Formation of fetal nerve fibers triggers Schwann cell proliferation due to the establishment of axonal association. Proliferating Schwann cells send its extended tips deeper into the bundle to encompass smaller bundles of axons through which axons are segregated. Finally, each Schwann cell selects an individual axon from the nerve bundle and

establishes a one-to-one relationship through a process called radial sorting. During this time, Schwann cells secrete basal lamina at the abaxonal surface of the Schwann cell/axon unit and laterally elongated Schwann cell plasma membrane spirally wraps the axons, forming the periaxonal space and the mesaxons. These fibers are known as promyelin fibers (Figure 1.4a). Eventually, these promyelin fibers differentiate into myelinated fibers in which compact myelin structure can be discriminated from non-compacted internal and external mexasons (Figure 1.4b) [5].

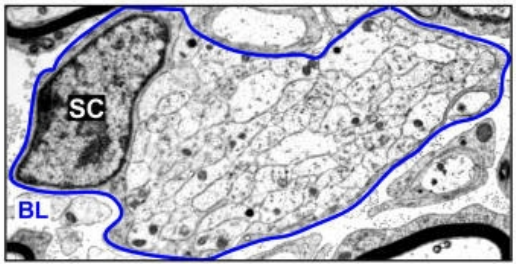

Figure 1.3. Fetal nerve fibers. Axon bundles are enveloped by a thin layer of Schwann cell membrane. SC: Schwann cell nucleus, BL: basal lamina [20].

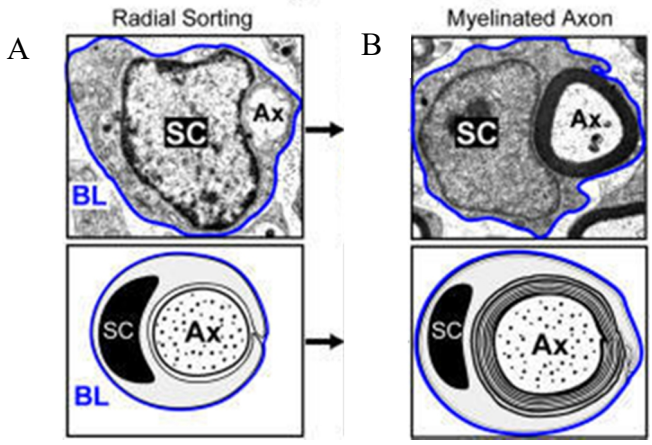

Figure 1.4. Radial sorting of an individual axon and myelination. (a) Promyelin nerve fibers generated during radial sorting. (b) Myelinated nerve fiber. SC: Schwann cell nucleus, BL: basal lamina, Ax: Axon. (adapted from Chan, 2007 [20]).

The mechanism of Schwann cell myelination is represented in Figure 1.5. The inner lip of the Schwann cell membrane laterally elongates and its spiral wrapping around axon forms new layers of myelin which are then compacted [5]

As a consequence of continuous Schwann cell proliferation and axonal segregation, only small caliber axon bundles remain unwrapped but they will eventually be transformed into Remark bundles by the wrapping of nonmyelinating Schwann cells [21].

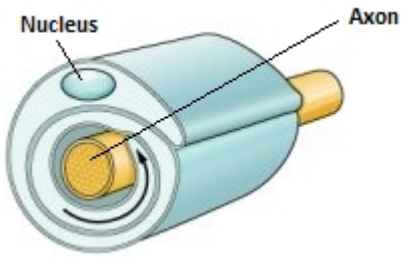

Figure 1.5. Myelin formation by the wrapping of the inner lip around axon.

1.2.2. Axon-Schwann Cell Interactions

The physical contact between axon and Schwann cell is established at an early stage of Schwann cell development. Although every Schwann cell has the potential to myelinate, only the ones that associate with large caliber axons differentiate into myelinating Schwann cells [5]. This is because of the survival factors, mitogens and differentiation signals secreted from the axons with which SCPs and mature Schwann cell interact [18]. Axonal interaction is not only required for the expression of myelin specific genes, but also for the continuation of a myelinating phenotype. When axon-Schwann cell interaction is lost, as in the case of nerve injury, the expression of myelin specific genes is downregulated [5].

Even though, there are numerous molecules that have been shown to have a role in the interaction between peripheral axons and Schwann cells, including MAG, $p75^{NTR}$, insulin-like growth factor 1 (IGF-1), integrin and transforming growth factor-beta 1 [2], the molecular mechanisms of such interaction remain poorly understood.

The neurogulin 1 (NRG1) and its receptors are accepted as the key regulators of axon-Schwann cell interaction at all stages of Schwann cell lineage and the myelination process. Neurogulin 1 is a growth factor which is expressed in spinal cord motor neurons, DRG sensory neurons, and autonomic neurons, while its receptors ErbB2 and ErbB3 are expressed on the Schwann cell. Thus, by binding its receptor on Schwann cell, axonal NRG1 mediate the interaction among axon and Schwann cell [22]. It has different functions during Schwann cell: (i) in early stages of development, they promote differentiation of neural crest cells into SCPs by inhibiting neural differentiation, (ii) it is important for the survival of SCPs, (iii) it promotes proliferation and migration of Schwann cells, (iv) it mediates the myelination process [23]. As well as the axonal diameter, NRG1 signaling also regulates the fate of immature Schwann cell whether they transform into myelinating or non-myelinating phenotype. The level of NRG1 type III derived signal determines the ensheatment fate of the axons [4]. The NRG1 type III is also responsible for the regulation of the myelin sheath thickness [22]. Studies performed in NRG1 mutant mice showed that heterozygous deletion (-/+) of NRG1 causes hypomyelination, whereas overexpression of it leads to hypermyelination. In the mouse mutant that has no NRG1, myelination does not occur [24] (Figure 1.6).

Figure 1.6. Myelination in mouse mutants lacking NRG1 (-/-), in heterozygous NRG1 (-/+) mice, and in transgenic mice overexpressing NRG1 [24].

Nectin-like (Necl) proteins are also shown to contribute to axon-Schwann cell interaction. Necl proteins are adhesion molecules that function in the adherent junctions and they contain three extracellular IgG-like domain, a transmembrane domain and a short cytoplasmic domain. Neurons and Schwann cells express different sets of Necl proteins. Myelinating Schwann cell principally express Necl4, whereas the axons express Necl1 and Necl2. By binding its glial partner Nec4 on Schwann cell, Necl1 mediates axon-Schwann

cell interaction along internodes (Figure 1.7) and this interaction is known to be essential for PNS myelination [25]. The disruption of the interaction between Necl1 and Necl4 molecules through the expression of dominant negative form of Necl4, or using their soluble extracellular domains, suppresses myelination [9].

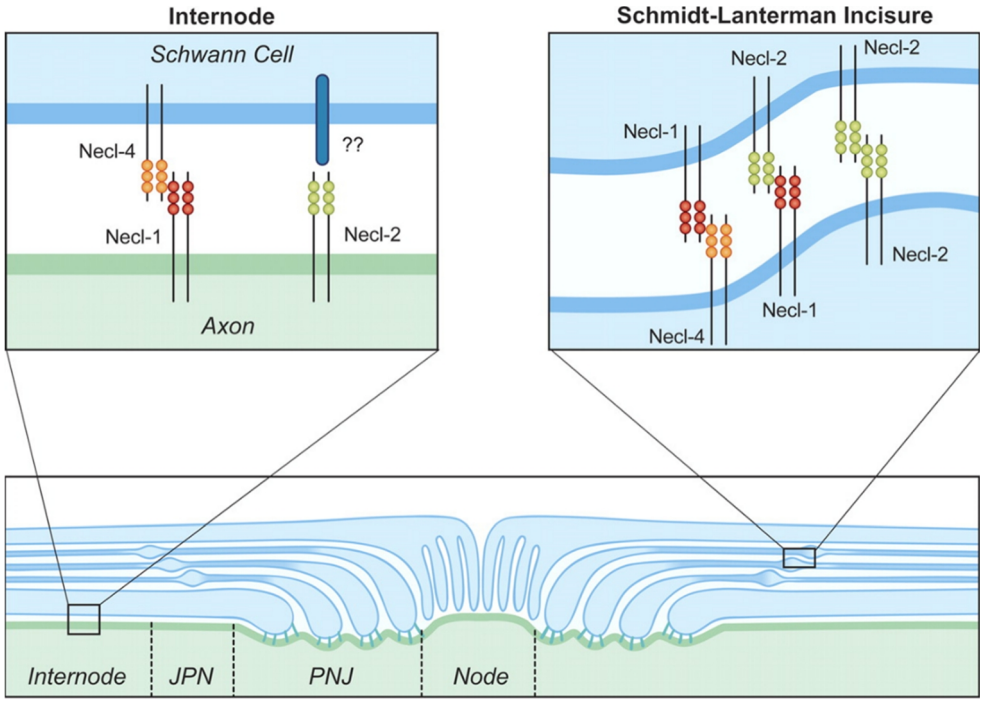

Figure 1.7. Nectin-like protein interactions in internodes and Schmidt-Lanterman incisures. Axonal Necl1 mediates axon-Schwann cell interaction by binding its glial partner Necl4. The glial partner of Necl2 is still not known [25].

1.2.3. Transcriptional Regulation of Myelination

After receiving the myelination signal from the axons, Schwann cell modifies their genetic expression program to allow the synthesis of myelin proteins. This regulation at the level of gene expression is mediated by transcription factors. Oct-6, Krox-20 and Sox-10 are the transcription factors that have been shown to contribute to the development of the myelinating phenotype of the Schwann cell.

Oct-6 is a POU domain transcription factor which is specifically expressed in the late stage Schwann cell precursors and promyelinating Schwann cell, but not in mature

myelinating Schwann cells. It represses the expression of late myelin proteins, MPZ and MBP. Thus, Oct-6 prevents immature Schwann cell from differentiating into myelinating phenotype by inhibiting the expression of end-stage myelin specific genes [5].

Krox-20 (EGR2) is a zinc-finger transcription factor that is activated in Schwann cell before the onset of myelination and required for the myelination of peripheral nerves. The expression of Krox-20 depends on continuous neuronal signaling *via* direct axonal contact. This transcription factor regulates the differentiation of Schwann cell by triggering the expression of myelin specific genes, MPZ and PMP22 [5, 26]. Both recessive and dominant mutations in Krox-20 are responsible for demyelinating or axonal types of CMT [27].

Transcription factor Sox-10 was shown to act during multiple consecutive stages of Schwann cell development in PNS. In addition to Schwann cell development, recent studies have demonstrated that Sox-10 is also required for Schwann cell differentiation and maintenance of the differentiated state [28].

1.3. Schwann Cell Remyelination

Schwann cells have an important ability that allows them to reverse their phenotype and dedifferentiate into the immature state when axonal contact is lost, making them one of the very few regenerative cells in our bodies [29, 30]. Due to peripheral nerve injuries, the interaction between axon and Schwann cell may be disrupted that leads to demyelination [31]. In response to axonal degeneration, Schwann cell downregulates the expression of genes related to myelinating phenotype while upregulating the expression of immature and nonmyelinating phenotype specific markers. This dedifferentiation allows Schwann cell to regain a proliferative-regenerating phenotype. When these reactive Schwann cells reestablish axonal contact, they can re-differentiate again into mature phenotype [29].

After a peripheral nerve injury, Schwann cells not only downregulate of myelin specific gene expressions, but also initiate fragmentation of compact myelin into small ovoids. Even though denervated Schwann cells are the major phagocytic cells during the early stages of demyelination, the final clearance of myelin debris is performed by phagocytic macrophages that are recruited to the injury site as a consequence of chemokine

and cytokine secretion from Schwann cells [32]. Therefore, the initial proliferation of Schwann cells plays a key role during the demyelination process [29]. Since degenerating myelin debris inhibits regeneration, remyelination can only begin after removal of all myelin debris [31]. A second phase of Schwann cell proliferation takes place during the remyelination period and enables the regeneration of peripheral nervous system [29].

Figure 1.8 shows schematic representation of demyelination and remyelination processes after a myelinopathic injury. The remyelinated nerves have often shorter internodal lengths and thinner myelin sheaths [33].

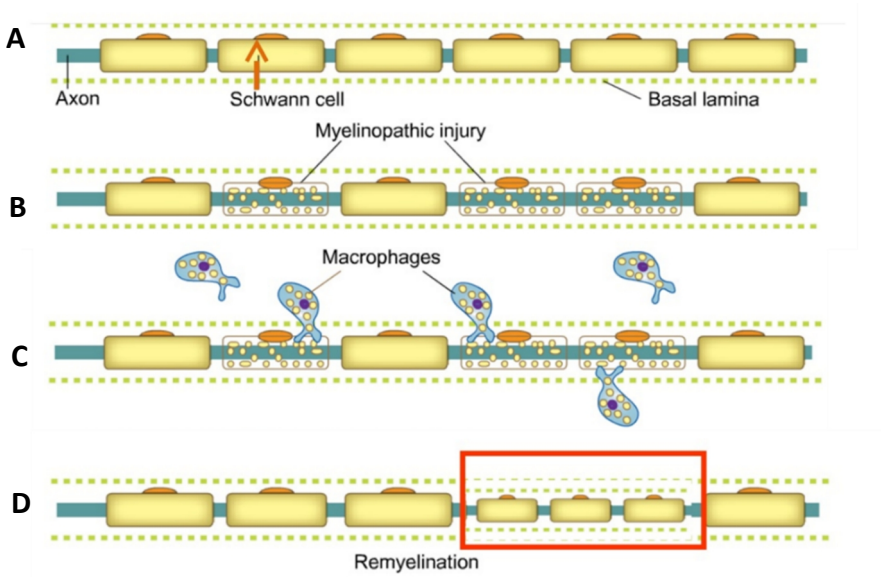

Figure 1.8. Schematic representation of demyelination and remyelination in PNS. (a) Normal myelinated nerve fiber. (b) Segmentally demyelinated nerve after a myelinopathic injury. (c) Macrophages recruited to demyelinated site are responsible for removing the myelin debris. (d) Remyelinated nerve fiber.

1.3.1. Molecular Mechanism of Schwann Cell Remyelination

After peripheral nerve injury, due to loss of the axonal contact, Krox-20 expression in myelinating Schwann cells is lost. Therefore, the expression of genes related to immature Schwann cell phenotype is regained [29]. Mitogen-activated protein kinases (MAPK), extracellular signal-regulated protein kinases (ERKs) and c-Jun N-terminal protein kinases (JNKs) are the signaling molecules that are activated during degeneration. The activation of

p38 MAPK molecule, as a result of an increase in the levels of neurogulin and FGF2 in the axons, induces demyelination. The downstream molecule activated by this signaling pathway is the transcription factor c-Jun that suppresses Krox-20 expression. c-jun is the principal regulator of Schwann cell injury response. It activates the repair program in Schwann cells and generates a cell specialized to favor regeneration [33]. The rapid activation of ERK 1/2 is also needed for the initiation of Schwann cell proliferation.

In addition to its involvement in almost all stages of Schwann cell development, NRG1 signaling is also important for degeneration and regeneration processes in PNS. NRG1 signaling inhibits myelination, induces myelin degradation and Schwann cell proliferation. Another molecule known to have upregulated expression after injury is FGF2.

The re-establishment of axon-Schwann cell interaction triggers remyelination. Recent studies have shown that in addition to developmental demyelination, NRG1 is involved also in the remyelination process and the expression of NRG1 type III is upregulated during remyelination. Apart from NRG1 and FGF2, IGF-1 and matrix metallopeptidase-9 (MMP-9) are known to take part in the remyelination process [33].

1.4. Lysolecithin-induced Demyelination

Lysolecithin (L-α-lysophosphatidylcholine or LPC) is a strong detergent substrate that is formed from phosphatidyl choline by the action of phospholipase A [34]. Due to its membrane dissolving function, injections of 1% solution of LPC induces focal demyelination both in PNS and CNS. It was first used by Hall and Gregson to create demyelinating lesion in the white matter of adult mouse spinal cord. After that, LPC has been used in several other species including cat, monkey, rat, and rabbit.

As a result of LPC injection, the myelin and the majority of myelin forming cells in the lesion area are rapidly removed. The most important feature of the lesion, created by LPC injection, is their ability to recover. In general, demyelination takes place immediately after the injection and almost all myelin debris is removed within 2-3 days. After loss of myelin debris, the lesion area is repopulated with glial cell precursors that proliferate and differentiate into glial cell and start remyelination. In rats and mice, depending on the age of

the animal and the injection area, remyelination starts between 7 and 14 days after LPC injection. Eventually, it is completed by 30 days after induction of the lesion [35].

1.5. Fibroblast Growth Factors

Fibroblast growth factors (FGFs) are a large family of polypeptide growth factors that have a molecular weight in the range of 17 to 34 kDa. They participate in diverse biological processes in mammalian tissues. Sequencing of human and murine tissue genomes has demonstrated presence of 22 members of FGFs (FGF1-FGF23) in each species, which are classified into seven subfamilies according to their sequence similarities and biochemical and developmental properties [36].

FGFs produce their biological effects *via* activation of fibroblast growth factor receptors (FGFRs). They bind to heparin or heparin sulphate for stabilization and this interaction is required for the activation of FGFRs effectively [37]. Most FGFs show similarity in terms of general protein structure, with an internal core region consisting of 28 highly conserved and six identical amino-acid residues. FGFR interaction is mediated by ten of these highly conserved residues. The conserved core region of FGF1 and FGF2 includes 12 antiparallel β-strands. Basic residues located in two of these β-strands create heparin binding sites on FGF2 (Figure 1.9) [38].

The majority of FGFs (FGFs 3 to 8, 10, 17 to 19, 21 and 23) carry an amino-terminal signal sequence that enables them to be easily secreted from cells. In contrast, FGF9, 16 and 20 do not have a cleavable amino-terminal sequence but, nevertheless, are secreted into the extracellular space. FGF1 and FGF2 also do not have signal peptides and they are not secreted like FGF9, 16 and 20, but instead are released from damaged cells or by an endoplasmic reticulum-Golgi independent exocytotic mechanism. Due to the lack of amino-terminal signal sequence, FGF11-14 remain in the cell and exert their effects in a receptor independent manner. Even though FGF22 has a signal peptide, they fail to be secreted and remain attached to the cell surface [39].

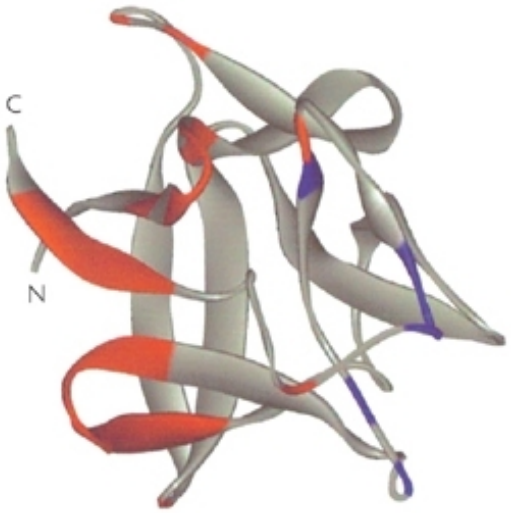

Figure 1.9. Three-dimentional structure of FGF2 protein showing receptor (red) and heparin binding sites (blue) [36].

1.5.1. FGF1 (Acidic FGF)

FGF1 is a 155 amino acid protein that is expressed both during development and adulthood [40, 41]. Similar to FGF2, FGF1 has a nuclear localization signal and it is shown to be associated with nucleus. The FGF1-induced mitogenesis depends on the presence of this nuclear localization signal. It may induce DNA synthesis without signaling through a cell surface receptor, which proposes that FGF1 may act through an intracrine mechanism with the help of its nuclear localization signal [40]. Recent studies have shown that deletion of its nuclear localization signal in neural cells inhibits both its nuclear localization and neurotrophic activity, including differentiation and cell survival. Thus, FGF1 may induce neural differentiation and protect cells from apoptosis directly *via* a nuclear pathway [41].

1.6. Fibroblast Growth Factor Receptors

FGFs mediate their biological effects in target cells by signaling through cell surface FGFRs, which belong to the tyrosine kinase receptor superfamily. FGFRs consist of three distinct domains: an extracellular ligand binding domain, a transmembrane domain and an intracellular tyrosine kinase domain. The extracellular domain includes two or three Ig-like

domains, a heparin binding domain and an acidic region. Ig-like II and Ig-like III domains are responsible for ligand binding.

FGF binding triggers dimerization of FGFRs and phosphorylation of cytoplasmic tyrosine residues that activates cytoplasmic signal transduction molecules [38]. Figure 1.10 shows the structure of FGFR and its dimerization through binding of both FGFs and heparin.

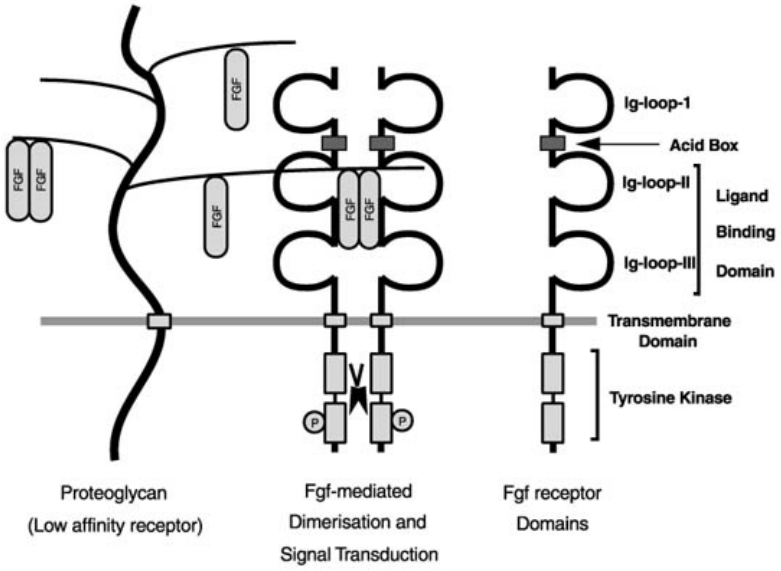

Figure 1.10. FGFR structure and dimerization after binding to FGFs and proteoglycan [42].

There are four different types of FGFRs: FGFR1, FGFR2, FGFR3 and FGFR4. Alternative splicing occurs within the region encoding C-terminal part of the third extracellular Ig-like loop and generates IIIb and IIIc isoforms of FGFR1-3 (Figure 1.11) [36]. Since third Ig-like domain is present in ligand binding region, alternative splicing in this region changes the ligand binding specificity of the receptor. Therefore, these alternatively spliced FGFR isoforms show different affinities for their ligands. FGF1 can bind to all these FGFR isoforms and also FGFR4 with similar affinities [39].

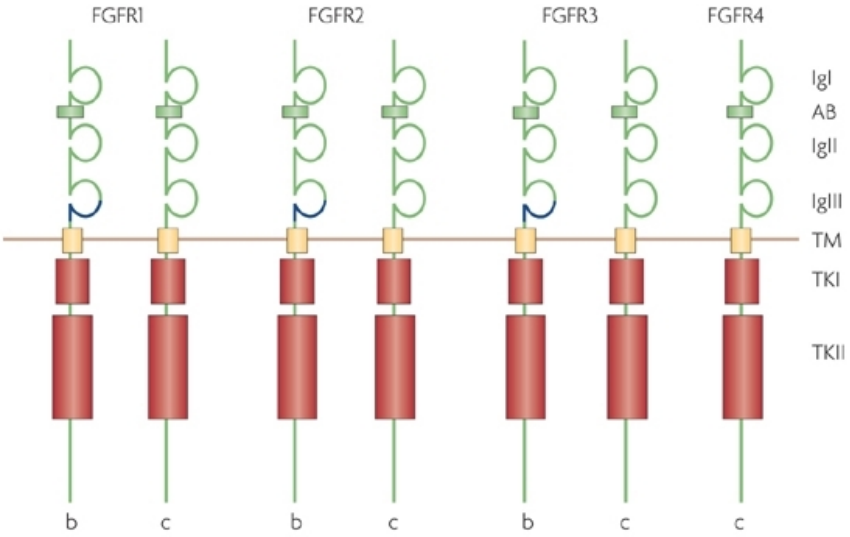

Figure 1.11. FGFR isoforms created through alternative splicing of the Ig-like III encoding region. FGFR4 has only one isoform [36].

1.7. Signaling Through FGFRs

Ligand binding to FGF receptors in conjunction with a heparin sulphate proteoglycan enables formation of the receptor complex that triggers autophosphorylation of its tyrosine kinase domains [39]. The signal is then transmitted through these autophosphorylated tyrosine residues either by docking adaptor proteins, which then facilitate the recruitment and activation of downstream signaling molecules, or by directly binding to signaling molecules [42].

Three major intracellular signaling pathways are shown to be activated through FGFRs including MAPK/ERK (mitogen-activated protein kinase/extracellular signal-regulated kinase), PLCγ/PKC (phosphoinositide phospholipase C/protein kinase C) and PI3K (phosphatidylinositol 3-kinase) pathways (Figure 1.12) [36]. MAPK/ERK pathway is associated with differentiation and survival in different cell types [43] and it is activated *via* docking of FGF receptor substrate 2 (FRS2)-Grb2-SOS complex. This complex then promotes the activation of RAS which ultimately activates ERK 1/2. Grb2 can also recruit Gab1 that is the responsible intracellular protein for the activation of PI3K and finally Akt/protein kinase B (PKB) pathway. Akt/PKC pathway is known to mediate the anti-apoptotic effects of FGFs in the developing nervous system [36]. PLCγ pathway, the third

major pathway, is activated by direct binding of PLCγ to Tyr766 of the receptor with its SH2 domain that enable the intracellular interaction with the receptor complex. Activated PLCγ hydrolyzes phosphatidylinositol into diacyglycerol (DAG) and inositol triphosphate 3 (IP3), DAG released by this process then activates PKC, while IP3 stimulates endoplasmic reticulum to release calcium. Mutation studies on Tyr766 have demonstrated that PLCγ/PKC pathway is not involved in FGFR-mediated mitogenesis and differentiation, however, it may have a role in cytoskeletal reorganization [39, 44].

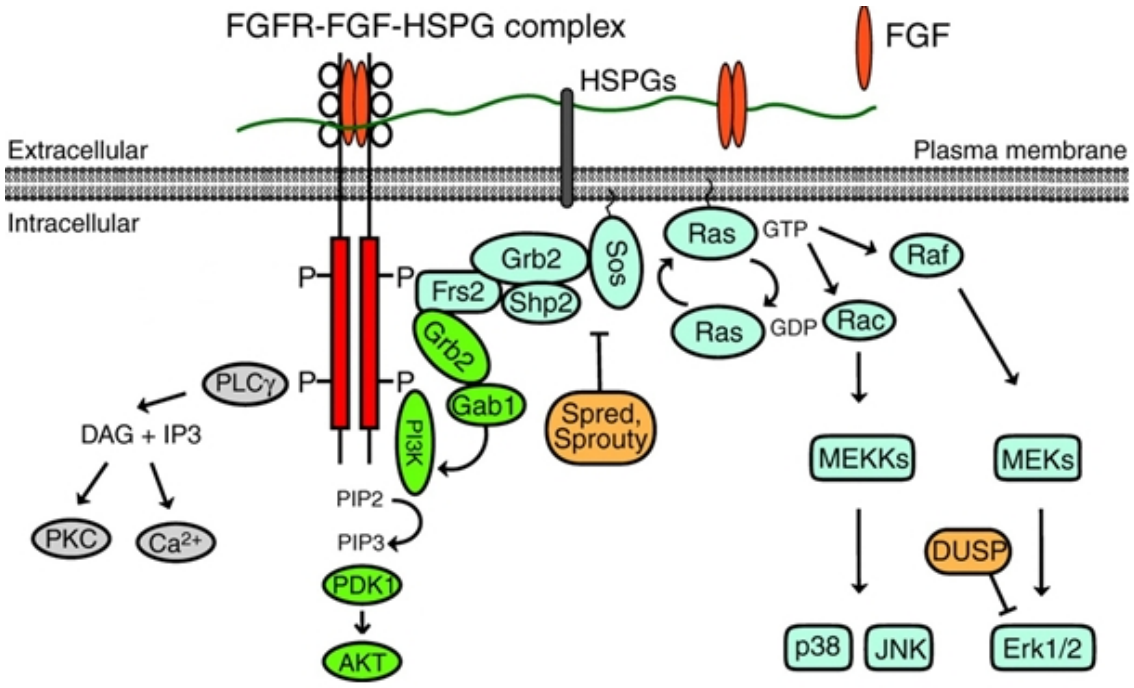

Figure 1.12. The FGF-FGFR signaling pathway. There are three main downstream pathways: PLCγ/PKC (1, grey), PI3K (2, green), and MAPK/Erk (2, blue) (Modified from Lanner and Rossant, 2010 [45]).

1.8. Fibroblast Growth Factors and Receptors in the Nervous System

A variety of experimental findings, coming from both *in vivo* and *in vitro* studies, have shown that FGFs regulates many aspects of the nervous system both during the development and adulthood [36]. During development, they have been found to control neurogenesis, axonal branching and differentiation. In the adulthood, on the other hand,

FGFs are involved in neuroprotection and repair processes following different brain and peripheral nerve lesions [38].

There have been lots of studies related to the expression patterns of FGFs and their receptors during CNS development. These studies have demonstrated that the prototypical FGFs, FGF1 and FGF2, are expressed both during development and adulthood, whereas FGF8 and FGF17 are only expressed during the early stages of proliferation and neurogenesis. Expression studies have also indicated that FGF1 and FGF2 show different expression patterns during CNS development. Although FGF2 is expressed by both neural and glial cells, FGF1 and FGF9 is mostly expressed by neural cells [46, 47].

Initial studies have shown that FGFR1 is expressed in both neuron and glia, whereas FGFR2 and FGFR3 are expressed predominantly in glial cells [48, 49]. The fourth member of FGFRs, FGFR4, was shown to be strongly expressed only during the early stages of CNS development, but not in adulthood except in the lateral habenular nucleus [38].

Expression and localization studies in CNS demonstrated the FGF1 may have a role during the maturation and maintenance of neurons [46]. In a different study, FGF1 was shown to promote the differentiation of oligodendrocyte precursor cells (OPCs) [50]. Furthermore, a recent study has showed that FGF1 promotes myelination and remyelination *in vitro* most likely through an indirect mechanism regulated by astrocytes [51].

Fibroblast growth factors have been studied less extensively in PNS compared to CNS. FGF2 is the only one that has been studied, but these studies are restricted to its role in peripheral nerve regeneration. After a nerve crush, both FGF2 protein and mRNA were shown to be upregulated at the lesion side and spinal ganglia. FGFR3 also showed a similar upregulation following lesion, suggesting a functional role of FGF2 via FGFR3 on neural survival [52]. Studies performed by using FGF2 and FGFR3 deleted mice demonstrated that FGF2 regulates injury-induced apoptosis through FGFR3 binding [53]. In contrast to FGFR3, the levels of FGFR1 and FGFR2 did not change after nerve crush and they were constitutively expressed at high levels. Therefore, it was suggested that FGF2 signaling via FGFR1/2 promotes Schwann cell proliferation and inhibits myelination [52].

1.8.1. Fibroblast Growth Factors and Receptors in Myelination

In recent years, a number of studies indicated the importance of FGF signaling both in myelination and remyelination period. For example, increased glial expression of FGF1 was shown to be involved in the regulation of CNS remyelination period by initiating an astrocyte dependent response [54]. FGF1 was also demonstrated to take part in the CNS myelination and remyelination processes again through regulating the inflammatory response genes in astrocytes that triggers the recruitment of oligodendrocyte precursors and initiation of remyelination [51]. Another study showed that conditional double mutant mice for FGFR1/2 in nonmyelinating Schwann cells had neuropathy in unmyelinated nociceptive sensory axons, suggesting the importance of FGFR signaling as potential mediators of axon-nonmyelinating Schwann cell interaction [55]. The same group demonstrated the significance of FGFR signaling in mature oligodendrocytes. Mice lacking both FGFR1 and FGFR2 in oligodendrocyte cell linages showed a normal proliferation and initiation of myelination, but a thin myelin sheath [56].

1.9. Previous Studies Performed in Our Laboratory

To investigate the possible role of FGF signaling during peripheral myelination period, in our laboratory it was performed expression analysis in mouse DRG tissue and sciatic nerve covering the postnatal developmental period, and localization analysis through immunolabelling on DRG culture, DRG tissue and sciatic nerve (Dağlıkoca, 2014). She also performed neutralization experiments in DRG culture.

Initially, she demonstrated that FGF1 and FGFR1-3 are expressed in DRG tissue through immunohistochemical stainings. To further delineate their expression in peripheral nervous system, and to provide evidence for their possible roles in myelination, she performed western analysis on total tissue lysates of the sciatic nerve from mice in different postnatal developmental stages. The results showed that FGF1 is expressed in the sciatic nerve after birth and its expression is upregulated during the myelination period and stabilized thereafter.

Her studies also demonstrated that the level of FGFR1 increases at P7 (postnatal day 7), about when axons start to be myelinated, and decreases at P10. After P10, its level increased again and stabilized in the adulthood, but at a lower expression level. FGFR2, on the contrary, was shown to be present in the sciatic nerve at high amounts until P10, and then reduced and stabilized. Although FGFR3 level increases at the start of myelination, it was at lower levels compared to that of FGFR1 and FGFR2.

Immunollabelling experiments on DRG culture showed that FGF1 is localized to neurons. Schwann cells were also shown to exhibit reactivity against FGF1 antibody, but only before axonal interaction. Moreover, localization studies performed on teased adult sciatic nerve samples and sciatic nerve cross sections supported the *in vitro* results implicating that FGF1 is localized to myelinated axons and nonmyelinating Schwann cells.

Furthermore, immunoblotting experiments both from DRG culture and sciatic nerve showed that all three receptors are localized to both free Schwann cells and Schwann cells interacting with axons. On the other hand, no FGFR was seen to be present in the neurons.

FGF1 localization to axons and FGFR1-3 to myelinating Schwann cells and their expressional upregulation during myelination period raised the question of whether if FGF1 has a role in the myelination process. To answer this question she has performed experiments in DRG culture and blocked FGF1 by a neutralizing antibody during the myelination period. These experiments implicated a reduction in the myelination in the absence of FGF1.

All these findings showed that FGF1 and its receptors may have a role in peripheral nervous system myelination but further investigations were required to confirm these findings and to unravel their exact roles. Therefore, in this study, we investigated the possible role of FGF1 and its receptors during myelination-remyelination through *in vivo* studies.

2. AIM OF THE STUDY

In vitro studies performed previously in our laboratory have demonstrated that FGF1 may have a possible role during peripheral nerve myelination (Dağlıkoca, 2014). Therefore, in this study we aimed:

- To further investigate the possible role of FGF1 in peripheral nerve myelination by *in vivo* studies.

- If it has a role in myelination, we aimed to investigate through which receptor (FGFR1, FGFR2 or FGFR3) FGF1 acts during peripheral this process.

To achieve these aims, initially, we performed a literature survey for the *in vivo* method and chose lysolecithin protocol that induces demyelination and promotes a remyelination period that is basically similar to developmental myelination. We used mouse sciatic nerve as an *in vivo* model of PNS.

We performed several experiments to reach our goals that can be summarized as follows:

(i) Lysolecithin injected nerves were investigated through immunohistochemistry in order to visualize demyelination after lysolecithin injection.

(ii) The time point for the initiation of remyelination was determined by western blot analysis for sciatic nerves dissected at different time points after lysolecithin injection.

(iii) The expression levels of FGF1 during the expected remyelination period after lysolecithin injection were investigated by western blot analysis, at different time points. Since FGF2 is known to be upregulated during peripheral nerve regeneration, it was used as a control in our experiments.

(iv) To investigate the role of FGF1 in PNS remyelination, it was blocked by injecting a neutralizing antibody during the remyelination period. The effect of FGF1 blocking on the expression levels of myelin proteins was then analyzed *via* western blotting.

(v) To examine the possible roles of FGFR1-3 in remyelination and to determine the receptor/receptors activated by FGF1 during this period, FGF receptors were blocked one by one through neutralizing antibody injection to the sciatic nerve during the remyelination period. To observe its effect, the expression levels of myelin proteins were investigated by western blot analysis. The expression of downstream molecules was also analyzed.

(vi) To further investigate through which FGF receptor FGF1 acts in the remyelination process, FGFR1, FGFR2 and FGFR3 were immunoprecipitated separately after FGF1 blocking and their phosphorylation levels were examined *via* western blotting.

3. MATERIALS

3.1. Mice Strain

Mice were provided by the animal facility in Bogazici University Center for Life Sciences and Technologies. The C57BL/6J mice strain was used in all experiments. They were kept under 12 hour light/ 12 hour dark conditions at 21 - 25 ºC and were given *ad libitum* access to food and water. All experimental procedures were carried out according to guidelines set by Bogazici University Ethics Committee.

3.2. Chemicals

Chemicals used in this study are listed in Table 3.1.

Table 3.1. Chemicals used in this study.

Chemical	**Supplier and Product Code**
1,4-Diazabicyclo[2.2.2]octane, 98% (DABCO)	Sigma-Aldrich, USA (D2,780-2))
2-Mercaptoethanol	Merck Millipore, USA (805740)
Acrylamide	Sigma, USA (A3553)
Ammonium peroxodisulphate (APS)	Fluka, Switzerland (09914)
Bovine Serum Albumin (BSA)	Sigma, USA (A2153)
DAPI	Roche, Germany (10 236 276 001)
EDTA	Riedel-de Haën, Germany (34549)
Fast Green FCF	Sigma, USA (F7252)
Glycerol	Sigma, USA (G5516)
Glycine	MP, USA (808822)
HCl	Merck, Germany (1003172500)
Methanol	Sigma-Aldrich, USA (32213)

Table 3.1. Chemicals used in this study. (cont.)

Chemical	Supplier and Product Code
N,N,N',N'-tetramethylethylenediamine (TEMED)	Sigma, USA (T7024)
N,N'-Methylenebisacrylamide	Sigma, USA (M7278)
Natrium deoxycholate	Merck, Germany (6504)
Paraformaldehyde (PFA)	Sigma-Aldrich, USA (15,812-7)
Phosphatase inhibitor cocktail tablets	Roche, Germany (04 906 845 001)
Protease inhibitor cocktail tablets	Roche, Germany (11 873 580 001)
Protein A-Agarose	Roche, Germany (11 134 515 001)
Sodium chloride	Merck Millipore, USA (106404)
Sodium dodecyl sulphate (SDS)	Sigma, USA (L3771)
Sodium hydroxide	Riedel-de Haën, Germany (06203)
Sucrose	Sigma, USA (S0389)
SuperSignal West Femto Maximum Sensitivity Substrate	Thermo Scientific, USA (34095)
Trisma base	Sigma, USA (T1503)
Triton X-100	Sigma, USA (T8787)
Tween-20	Riedel-de Haën, Germany (63158)
Western blotting luminol reagent	Santa Cruz, USA (sc-2048)

3.3. Buffers and Solutions

Buffers or solutions for western analysis and their contents are given in Table 3.2.

Table 3.2. Buffers or solutions for western blot analysis.

Buffer or Solution	Content
10 % SDS polyacrylamide gel (running)	375 mM Tris-Cl (pH 8.8)
	10 % Acrylamide:Bisacrylamide (37.5:1)

Table 3.2. Buffers or solutions for western blot analysis. (cont.)

Buffer or Solution	Content
10 % SDS polyacrylamide gel (running) (cont.)	0.1 % SDS
	0.1 % APS
	0.1 % TEMED
	0.001 M EDTA
12.5 % SDS polyacrylamide gel (running)	375 mM Tris-Cl (pH 8.8)
	12.5 % Acrylamide:Bisacrylamide (37.5:1)
	0.1 % SDS
	0.1 % APS
	0.1 % TEMED
	0.001 M EDTA
2 X Protein Sample Buffer	100 mM Tris-Cl
	4 % SDS
	0.2 % bromophenol blue
	20 % glycerol
	200 mM 2-mercaptoethanol
4.5 % SDS polyacrylamide gel (stacking)	125 mM Tris-Cl (pH 6.8)
	4.5 % Acrylamide:bisacrylamide (37.5:1)
	0.1 % SDS
	0.1 % APS
	0.1 % TEMED
	0.001 M EDTA
Blocking Solution	5 % bovine serum albümin or 5 % skim milk powder in TBST
Radio-immuno-precipitation assay (RIPA) Buffer	1 M NaCl
	1 % Triton X-100
	0.1 % Na-deoxycholate
	50 mM Tris-Cl (pH 7.4)
	2 mM EDTA

Table 3.2. Buffers or solutions for western blot analysis. (cont.)

Buffer or Solution	Content
Radio-immuno-precipitation assay (RIPA) Buffer (cont.)	0.1 % SDS
	Mini protease inhibitor cocktail
	Phosphatase inhibitor cocktail
Running Buffer	25 mM Tris
	250 mM Glycine
	0.2 % SDS
Stripping Solution	62.5 mM Tris-Cl (pH6.8)
	2 % SDS
	0.7 % 2-mercaptoethanol
TBS with Tween-20 (TBST)	0.1 % Tween-20 in 1X TBS
Transfer Buffer	25 mM Tris
	200 mM Glycine
	20 % Methanol
Tris Buffered Saline (TBS)	20 mM Tris-Cl (pH 8.0)
	150 mM NaCl

Buffers and solutions used for tissue processing and immunohistochemistry are given in Table 3.3. Phosphate-buffered saline (PBS) used for preparation of these buffers and solutions was obtained from GIBCO (USA).

Table 3.3. Buffers or solutions used for tissue processing and immunohistochemistry.

Buffer or Solution	Content
Blocking Solution	0.25 % Triton X-100
	0.25 % BSA in 1X PBS
DABCO mounting medium	2.5 % DABCO
	50 mM Tris-Cl (pH 8.0)
	90 % Glycerol

Table 3.3. Buffers or solutions used for tissue processing and immunohistochemistry. (cont.)

Buffer or Solution	Content
DAPI	0.02 µg/ml in 1X TBS
Paraformaldehyde Solution	4 % PFA in 1X PBS
Sucrose Solution	20 % sucrose in 1X PBS
Washing Solution	0.25 % Triton X-100 in 1X PBS

3.4. Antibodies

Primary and secondary antibodies used for western blot analysis are listed in Table 3.4 and 3.5, respectively. Information about host, dilution and product code are also provided in these tables.

Table 3.4. Primary antibodies used for western blot analysis.

Primary Antibody	Host	Dilution	Supplier and Product Code
Actin	Goat	1:1000	Santa Cruz Biotechnology (sc-1616)
ERK 2	Rabbit	1:1000	Santa Cruz Biotechnology (sc-154)
FGF1	Goat	1:1000	Santa Cruz Biotechnology (sc-1884)
FGF1	Rabbit	1:1000	Abcam (ab76662)
FGFR1	Rabbit	1:1000	Santa Cruz Biotechnology (sc-121)
FGFR2	Rabbit	1:1000	Santa Cruz Biotechnology (sc-122)
FGFR3	Rabbit	1:1000	Santa Cruz Biotechnology (sc-123)
MAG	Rabbit	1:1000	Santa Cruz Biotechnology (sc-15324)
MBP	Mouse	1:1000	Sternberger monoclonals (SMI-94R)
p-AKT (Ser473)	Rabbit	1:2000	Cell Signaling (4060)
Pan-Akt	Rabbit	1:1000	Cell Signaling (4691)
p-ERK 1/2	Rabbit	1:2000	Cell Signaling (4370)

Table 3.4. Primary antibodies used for western blot analysis. (cont.)

Primary Antibody	Host	Dilution	Supplier and Product Code
p-FGFR (Tyr653/654)	Rabbit	1:1000	Cell Signaling (3471)
PLC gamma 1	Rabbit	1:1000	Cell Signaling (2822)
p-PLC gamma 1 (Tyr783)	Rabbit	1:1000	Cell Signaling (2821)

Table 3.5. List of secondary antibodies used for western blot analysis.

Target	Host	Tag	Dilution	Supplier and Product Code
Goat	Donkey	Horse Radish Peroxidase	1:5000	Santa Cruz Biotechnology (sc-2020)
Mouse	Donkey	Horse Radish Peroxidase	1:5000	Santa Cruz Biotechnology (sc-2314)
Rabbit	-	Horse Radish Peroxidase	1:3000	Cell Signaling (7074)

Primary antibodies that have been used for immunohistochemistry are listed in Table 3.6.

Table 3.6. Primary antibodies used for immunohistochemistry.

Antigen	Host	Dilution	Supplier and Product Code
MBP	Mouse	1:1000	Sternberger monoclonals (SMI-94R)
MBP	Chicken	1:200	Abcam (ab9348)
Na Channel	Mouse	1:3000	Sigma (S8809)
NF-200	Rabbit	1:1000	Sigma Aldrich (N4142)

Table 3.6. Primary antibodies used for immunohistochemistry. (cont.)

Antigen	Host	Dilution	Supplier and Product Code
NF-200	Mouse	1:200	Santa Cruz Biotechnology (sc-32729)

Secondary antibodies that have been used for immunohistochemistry are given in Table 3.7.

Table 3.7. Secondary antibodies used for immunohistochemistry.

Target	Host	Fluorescent Tag	Dilution	Supplier and Product Code
Mouse	Donkey	Alexa 488	1:500	Molecular Probes (A21202)
Mouse	Donkey	Alexa 555	1:500	Molecular Probes (A31570)
Rabbit	Donkey	Alexa 488	1:500	Molecular Probes (A21206)
Rabbit	Donkey	Alexa 555	1:500	Molecular Probes (A31572)
Chicken	Goat	Alexa 488	1:500	Dako
Chicken	Goat	Dy488	1:500	Abcam (ab96947)
Donkey	Chicken	FITC	1:200	Jackson

Neutralizing antibodies that have been used for injections are listed in Table 3.8. List of isotype control immunoglobulins used for injections are also provided in Table 3.9.

Table 3.8. Neutralizing antibodies used in this study.

Target	IgG class	Supplier and Product Code
FGFR1 (IIIb isoforms)	Mouse IgG_1	R&D Systems (MAB765)
FGFR2	Mouse IgG_1	R&D Systems (MAB684)
FGF1	Rabbit IgG	Abcam (ab9588)
FGFR3	Rat IgG_{2A}	R&D Systems (MAB710)

Table 3.9. Isotype control immunoglobulins used in this study.

Immunoglobulin	Supplier and Product Code
Mouse Monoclonal IgG_1	R&D Systems (MAB002)
Rat Monoconal IgG_{2A}	R&D Systems (MAB006)
Rabbit IgG	Abcam (ab37415)

3.5. Disposable Materials

Disposable materials that have been used in this study are listed in Table 3.10.

Table 3.10. Disposable materials used in this study.

Material	Producer
Centrifuge tubes, 15 ml	Axygen Scientific, USA
Centrifuge tubes, 50 ml	Axygen Scientific, USA
Fitered tips	Axygen Scientific, USA
Pipette tips	Axygen Scientific, USA
Microscope cover glass	Isolab, Germany
Positively charged slides	Thermo Scientific, USA
Pasteur pipettes	Isolab, Germany
Microcentrifuge tubes, 0.5 ml	Axygen Scientific, USA
Microcentrifuge tubes, 1.5 ml	FIRATMED, Turkey
Microcentrifuge tubes, 2 ml	Axygen Scientific, USA

3.6. Equipment

The list of laboratory equipment used throughout this project is given in Table 3.11.

Table 3.11. Laboratory equipment used in this study.

Equipment	**Producer**
Autoclave	Astell Scientific, UK
Blotting Apparatuse	Mini Trans-Blot Cell, Bio-Rad, Italy
Centrifuge	Centrifuge 5415 R, Eppendorf, USA Spectrafuge 16M, Labnet, USA
Confocal microscopy system	TCS SP5, Leica Microsystems, USA
Cryostat	Leica CM3050 S, USA
Deep Freezers	-20 ºC Arçelik, Turkey
Documentation System	Raytest Stella, Bio-Rad, USA
Electrophoresis	Mini-Protean III Cell, Bio-Rad, Italy
Fluorescence stereomicroscope	MZ16FA, Leica Microsystems, USA
Heat blocks	DRI-Block BD-2A, Techne, UK
Homogenizer	MagNa Lyser, Roche, Germany
Illuminator	41723-Series High Intensity Illuminator, Cole Parmer, USA
Magnetic stirrer	Speed Safe Hanna Instruments, USA
Micropipettes	Gilson, USA
Microscope	S2026, Prior, UK
Microwave oven	Arçelik, Turkey
Power supplies	PowerPac Basic, Bio-Rad, Italy
Refrigerator	+4 ºC Arçelik, Turkey
Shaker	SL 350 Nüve, Turkey
Spectrophotometer	NanoDrop ND-1000 NanoDrop, USA
Ultra Low Temperature Freezer	-86 ºC Thermo Forma, USA
Vortex	NM110 Nuve, Turkey

4. METHODS

4.1. Sciatic Nerve Injection

Sciatic nerve injections were performed as described by *Gonzalez et al.* (2014). Mice were anesthetized by using isofluorane inhalation system. Oxygen flow to anesthesia induction box was adjusted to 1% liters/min and isofluorane system was turned on to 3 % (volume/volume). Mask anesthesia system was used. The mouse's nose was placed into the mask cone and its tail and paw reflexes were checked by pinching to ensure that complete anesthesia has been reached. The incision region was prepared for surgery by shaving with razor blade and by applying Baticon with sterile cotton swabs. Anesthesia was maintained by reducing isoflurane to 1.5-2% (volume/volume). The skin was cut parallel to the nerve with a scissors and the gluteus superficialis and biceps femoris were exposed. The connective tissue that connect the muscles was cut with a scissors. In order to gently lift the sciatic nerve out, a forceps were used. Injections to the nerve were achieved by using a 33 ga Hamilton syringe. After injection, the sciatic nerve was replaced back to the bottom of the cavity and the muscles were replaced on top of the nerve. Muscles did not need sutures, since they were not cut. The skin was closed with surgical sutures. After injections, mice were kept in separate cages.

4.2. Lysolecithin Induced Demyelination

Lysolecithin was dissolved in sterile 0.9% NaCl solution to prepare 2% solution, and used to induce demyelination in the sciatic nerve of mice. For this purpose, mice were anesthetized and the sciatic nerve was exposed as previously described in section 4.1. Nerve was injected with 5 µl 2% lysolecithin solution using a 33 ga Hamilton syringe. In order to observe filling of each nerve, 0.05% Fast Green FCF was included in lysolecithin solution. After injection, the needle was left in the sciatic nerve for about 1 minute to prevent leakage of the injected solution. For all demyelination experiments, left sciatic nerve was injected with lysolecithin solution, and right sciatic nerve was identically injected with an equal volume of 0.9% NaCl solution containing 0.05% Fast Green FCF. Mice were allowed to recover until sacrification.

To ensure about demyelination and to determine the starting day for remyelination, mice were sacrificed via carbon dioxide inhalation after 1, 7, 15 and 21 days from lysolecithin injection. The sciatic nerves were dissected and total protein was isolated for western blot analysis. The expression levels of MAG, MBP, FGF1 and FGF2 were investigated and all experiments were performed in triplicates.

A second group of mice were used for immunohistochemistry. Sciatic nerves from mice that were killed at 7^{th}, 14^{th} and 28^{th} day after lysolecithin injection were fixed and immunolabelled for MBP and NF. These experiments were also performed in triplicates.

4.3. Antibody Mediated FGF1 Blocking

FGF1 was blocked *in vivo* by using a neutralizing antibody (Abcam ab9588) in order to investigate the role of FGF1 during the remyelination process after lysolecithin injection. Mice were anesthetized 8 days and 12 days after original lysolecithin injection and the exposed sciatic nerves were injected with 5 µl of 40 µg/ml Rabbit IgG or anti-FGF1 neutralizing antibody diluted in 1X PBS containing 0.05% Fast Green FCF. The incision site were then closed with surgical sutures and mice were returned to cages for recovery. Finally, 14 days after the initial injection of lysolecithin, the mice were sacrificed, the sciatic nerves were collected and total protein is isolated. The samples were kept on ice to be used for western Blot analysis and immunoprecipitation assays.

The tissues collected for western blot analysis were used for the evaluation the major myelin proteins, MAG and MBP. The tissues collected for immunoprecipitation were used for the precipitation of FGFR1, FGFR2 and FGFR3 one by one and phosphorylation levels of these proteins were investigated using Western analysis. The experiment was performed in triplicates both for western blot and immunoprecipitation.

4.4. Antibody Mediated FGFR1, FGFR2 and FGFR3 Blocking

After lysolecithin injection, blocking of FGFR1, FGFR2 or FGFR3 was achieved *via* neutralizing antibody injection.

Mice were anesthetized at day 8, and again at day 12, after initial injection of 5 µl 2% lysolecithin and their sciatic nerves were exposed. For FGFR1 blocking, left sciatic nerve was injected with 5 µl of 100 µg/ml Mouse IgG1, while right sciatic nerve was injected with anti-FGFR1 neutralizing antibody (R&D Systems, MAB765). For FGFR2 blocking, left sciatic nerve was injected with 5 µl of 100 µg/ml Mouse IgG1, while right sciatic nerve was injected with anti-FGFR2 neutralizing antibody (R&D Systems, MAB684). Finally, for FGFR3 blocking, left sciatic nerve was injected with 5 µl of 200 µg/ml Rat IgG2A, while right sciatic nerve was injected with anti-FGFR3 neutralizing antibody (R&D System, MAB710). Three mice were used for each FGF receptor. The injected control IgGs and neutralizing antibodies were diluted in 1XPBS including 0.05% Fast Green FCF. The incision sites were then closed with surgical sutures, and mice were allowed to recover in separate cages. After 14 days from initial lysolecithin injection, mice were sacrificed, their sciatic nerves were dissected and total protein was isolated. The protein samples were used in western blot analysis to study the expression levels of MAG and MBP. Furthermore, expression of signaling molecules, namely p-AKT, p-ERK and p-PLC gamma 1 were analyzed.

4.5. Preparation of Sciatic Nerve Tissue Homogenate

Sciatic nerves were dissected with clean tools and were placed on ice. For 10 mg tissue, 100 µl of RIPA buffer was added together with enough number of MagnaLyser ceramide beads. The nerves were then homogenized by using MagnaLyser homogenizer at 6500 rpm for 60 seconds. Lysed sample were centrifuged in a bench-top centrifuge for 20 minutes with the setting of 13.200 rpm at 4ºC. The supernatant including total protein extract was transferred to a new tube. By using bicinchoninic acid protein assay kit (Pierce, USA), total protein concentration was determined.

4.6. Immunoprecipitation

Sciatic nerve homogenate was completed to approximately 500 µl with RIPA buffer and 0.25 µg of the appropriate control IgG (corresponding to the host species of the primary antibody) was added into the solution. Thirty µl Protein A-Agarose bead were washed three times with RIPA and the tissue homogenate was transferred on washed agarose beads. It was

then incubated at 4ºC for 30 minutes on a rotating device. After incubation, it was centrifuged for 3 minutes at 13.200 rpm. Supernatant was transferred to a new microcentrifuge tube. BCA assay was performed to determine the concentration of the protein. Concentration of all samples were adjusted approximately to 600 µg/ml and their volumes were equalized with RIPA buffer. Ten µl of primary antibody was added into precleared lysates and incubated at 4ºC for 2 hours with mixing on a rotating device. 40 µl Protein A-Agarose beads were washed three times with 300 µl RIPA buffer. After each wash, beads were pelleted with centrifugation at 13.200 rpm for 1.5 minutes. Following lysate-antibody incubation, it was transferred into washed agarose beads and incubated overnight at 4ºC with mixing on a rotating device. Pellet was collected by centrifugation at 13.200 rpm for 3 minutes at 4ºC. Supernatant was carefully aspirated and discarded. Pellet was then washed three times with RIPA buffer and each time centrifugation step described above was repeated. After final wash, supernatant was aspirated and discarded, and pellet was re-suspended in 40 µl of 2X electrophoresis sample buffer. Samples were boiled for 5 minutes at 95ºC and were again centrifuged at 13.200 rpm for 3 minutes. All of the supernatant was used for western blot analysis through which expression of p-FGFR1, p-FGFR2 and p-FGFR2 were evaluated.

4.7. Western Blot Analysis

Ten µg of sciatic nerve lysate was mixed with 2X protein sample buffer to investigate the expression of myelin proteins. Hundred µg of sciatic nerve lysate was mixed with 6X protein sample buffer for western analysis of other proteins. Samples were incubated at 95ºC for 5 minutes to denature proteins. Equal amounts of samples were then loaded into the wells of 12.5% SDS polyacyrlamide gels. Samples were run at 80 V until they reached the separating gel, after which they were run at 100 V for about 2 hours. Proteins, which were separated on gel according to their size, were electroblotted to polyvinyl difluoride (PVDF) membranes (Roche, Germany) at 100 V in transfer buffer for 15-155 minutes depending on the size of the protein of interest (1 minute per 1 kDa). After transfer, membrane was rinsed three times with 1XTBST for 5 minutes each. It was blocked with blocking solution for 1 hour on a rotating device at room temperature. The membrane was then incubated with primary antibody diluted in 1% or 5% blocking solution overnight at 4ºC with gentle agitation. The membrane was rinsed three times with 1XTBST for 5 minutes to remove

excess antibody. Horseradish peroxidase (HRP)-conjugated secondary antibody incubation was performed at room temperature for one hour. Subsequent to washing 5 minutes with 1XTBST for three times and incubating the membrane in Lumi-Light Western blotting substrate (Roche, Germany) for one minute, the blots were visualized by chemiluminescence detection system (Stella, Germany). Actin protein was used for normalization of the expression levels of the investigated proteins.

4.8. Tissue Processing and Imunohistochemistry

Sciatic nerve tissues were dissected and fixed with 4% cold PFA for 1 hour. After washing 10 minutes with 1XPBS for three times, the tissues were dehydrated via incubation with 20% sucrose in 1XPBS overnight. Dehydrated sciatic nerve tissues were placed into embedding mold containing OCT medium and frozen at -80^{o}C. Frozen sciatic tissues were cut into 12 µm longitudinal sections using a cryostat. Sections were taken onto commercial positively charged slides, air dried, and frozen at -80^{o}C freezer until immunolabelling.

Frozen slides were left at room temperature for about 20 minutes before use for immunolabelling experiments. Afterwards, the sections were rehydrated by washing three times with 1XPBS for 10 minutes. They were then blocked with blocking solution for 1 hour at room temperature. Following blocking, each section was incubated overnight with the primary antibody diluted in blocking solution in a humidified chamber at 4^{o}C. In order to remove excess primary antibody, sections were rinsed 10 minutes with washing solution for three times. Incubation with fluorescent dye conjugated secondary antibody (diluted in blocking solution) was performed for 1 hour at room temperature. For DAPI labelling, samples were incubated with 0.02 µg/ml DAPI in 1XTBS for 5 minutes. After final 10 minutes wash with washing solution for three times, samples were mounted using DABCO fluorescent protecting mounting medium and stored at 4^{o}C, at dark until visualization. Eventually, they were visualized using fluorescence microscope.

4.9. Statistical Analysis

All statistical analyses were performed using GraphPad Prism version 6.05. Differences in protein expression between experimental groups were statistically analyzed

using Student's t-test or one-way ANOVA. The level of significance was chosen as 0.05 or 5 % ($p < 0.05$).

5. RESULTS

Expression and localization studies performed previously in our laboratory (Dağlıkoca, 2014) demonstrated that FGF1, FGF2 and FGF receptors FGFR1-3 were all expressed in dorsal root ganglia (DRG) co-cultures and sciatic nerve. It was reported that FGF1 was localized to axons and non-myelinating Schwann cells, whereas FGFR1, 2 and 3 were localized only to Schwann cells in adult mice. Since axon-Schwann cell interaction is the key for the myelination process, it can be hypothesized that FGF1 produced in neurons can potentially be released by axons and act on Schwann cells, through which it may induce myelination. It was shown that myelination is reduced after FGF1 blockage with a neutralizing antibody in DRG co-cultures (Dağlıkoca, 2014). To confirm these findings by *in vivo* studies and also to further investigate FGF1-receptor interaction during the myelination process, PNS remyelination procedure was used in this study. Adult mouse sciatic nerve was initially demyelinated by lysolecithin injection, and the potential roles of FGF1 and FGFR1-3 were investigated by blocking them during the remyelination period with direct injection of a neutralizing antibody to the mice sciatic nerve.

5.1. Injection of 2% LPC Solution Induces Demyelination in Mouse Sciatic Nerve

To visualize demyelination after lysolecithin injection, sciatic nerves were dissected one day after the injection and frozen sections were prepared. They were then immunolabeled with antibodies specific to myelin basic protein (MBP) that is used as a myelin marker and neurofilament (NF) used as a neuronal marker.

As seen on Figure 5.1, myelin sheath of normal adult mouse sciatic nerve had a well-defined fibrillary like structure. Furthermore, axons were smoothly surrounded by myelin sheath.

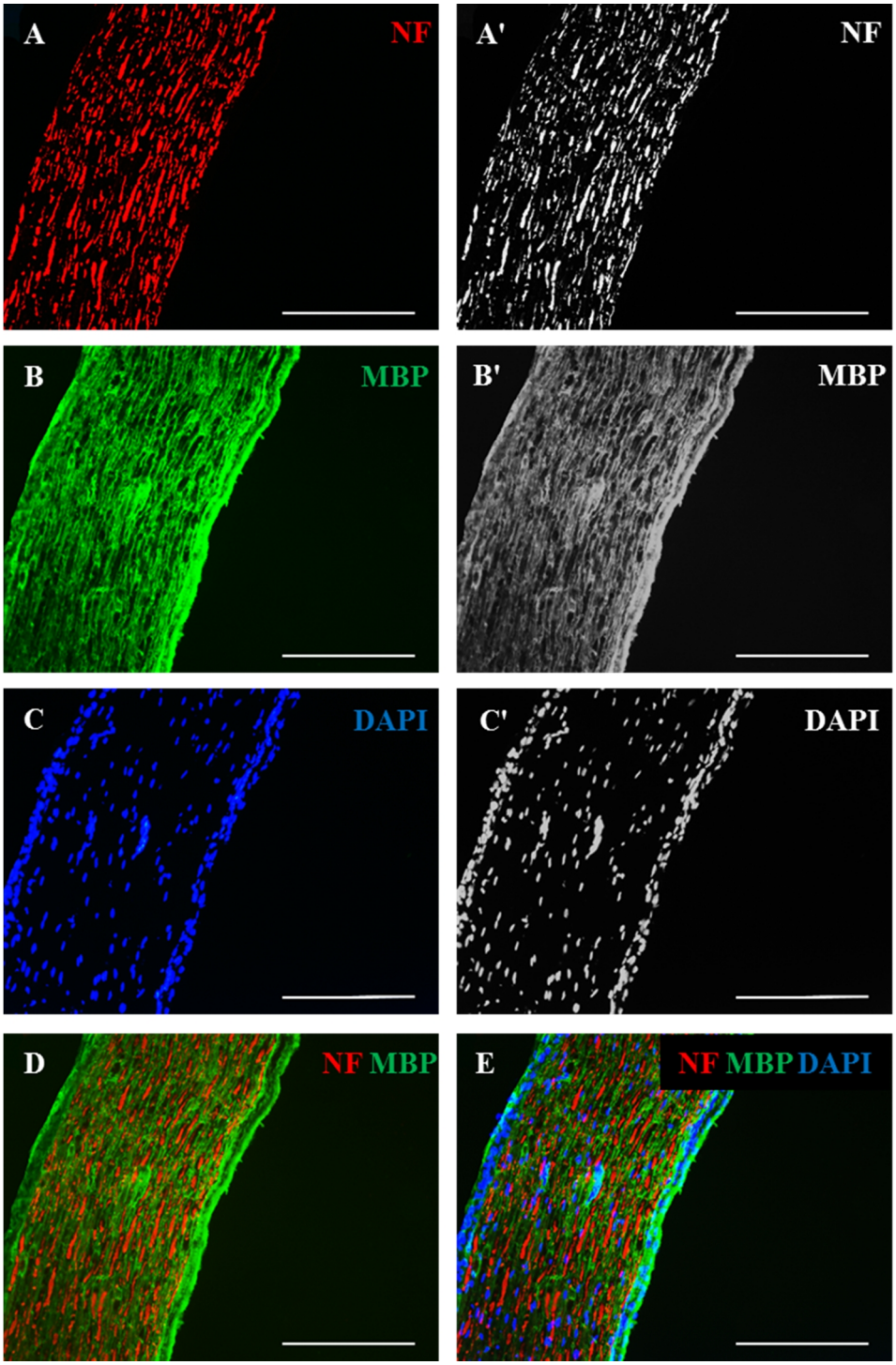

Figure 5.1. Immunolabelling of adult mouse sciatic nerve for NF (a) and MBP (b). DAPI staining shows Schwann cell nuclei (c). Axons are located in myelin sheath (d, e). Scale bars represent 200 µm.

Figure 5.2, on the other hand, shows adult mouse sciatic nerve injected with 1% of lysolecithin solution. Myelin sheath was seen to be locally demyelinated one day after lysolecithin injection.

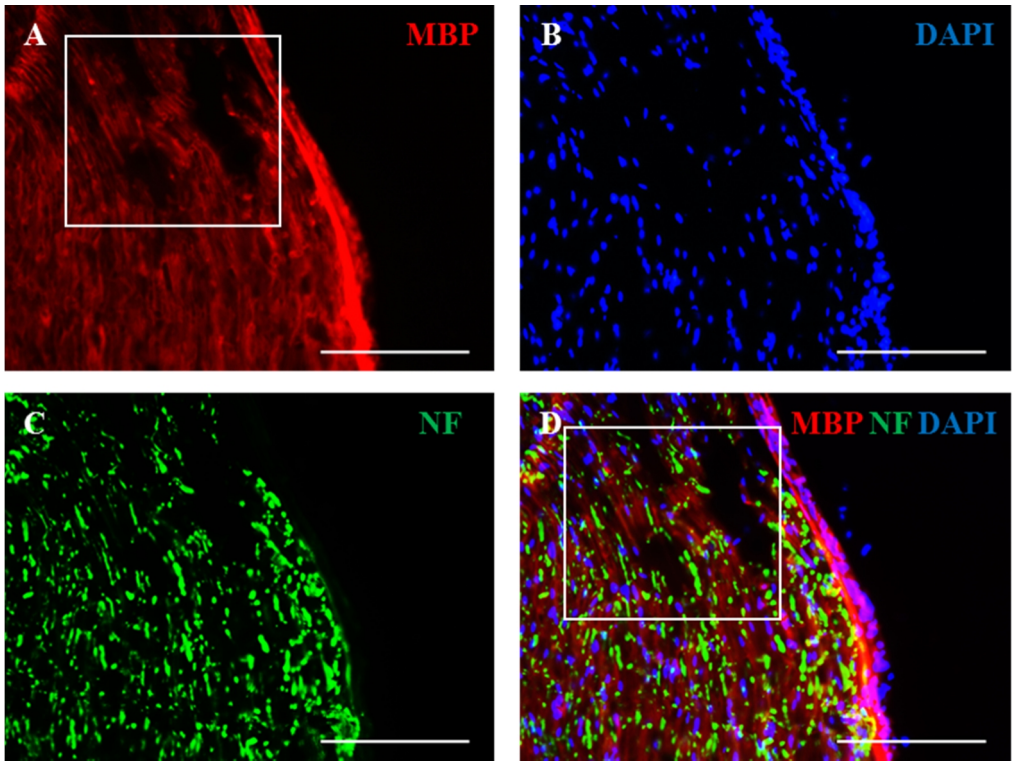

Figure 5.2. Immunolabelling of adult mouse sciatic nerve injected with 1% of lysolecithin solution for MBP (a) and NF (c). DAPI staining shows Schwann cell nuclei (b). Merge of myelin staining, NF and DAPI is shown in d. Prominent areas of myelin pallor (encircled with a square) is seen (a, d). Scale bars represent 100 µm.

In order to increase the effect of lysolecithin, in other words to demyelinate the sciatic nerve almost totally, the concentration of lysolecithin was increased to 2% and the experiment was repeated.

Sciatic nerve consists of afferent and efferent fibers, which are sensory and motor fibers, respectively. Because of the layer between these fibers, only one of them can be injected with solution. Immunohistochemical staining on Figure 5.3(a, a', and c) shows myelin structure difference between injected and non-injected fibers. Myelin sheath of the

injected fiber had lost its fibrillary structure compared to the non-injected one. Myelin was dissolved as a result of demyelination.

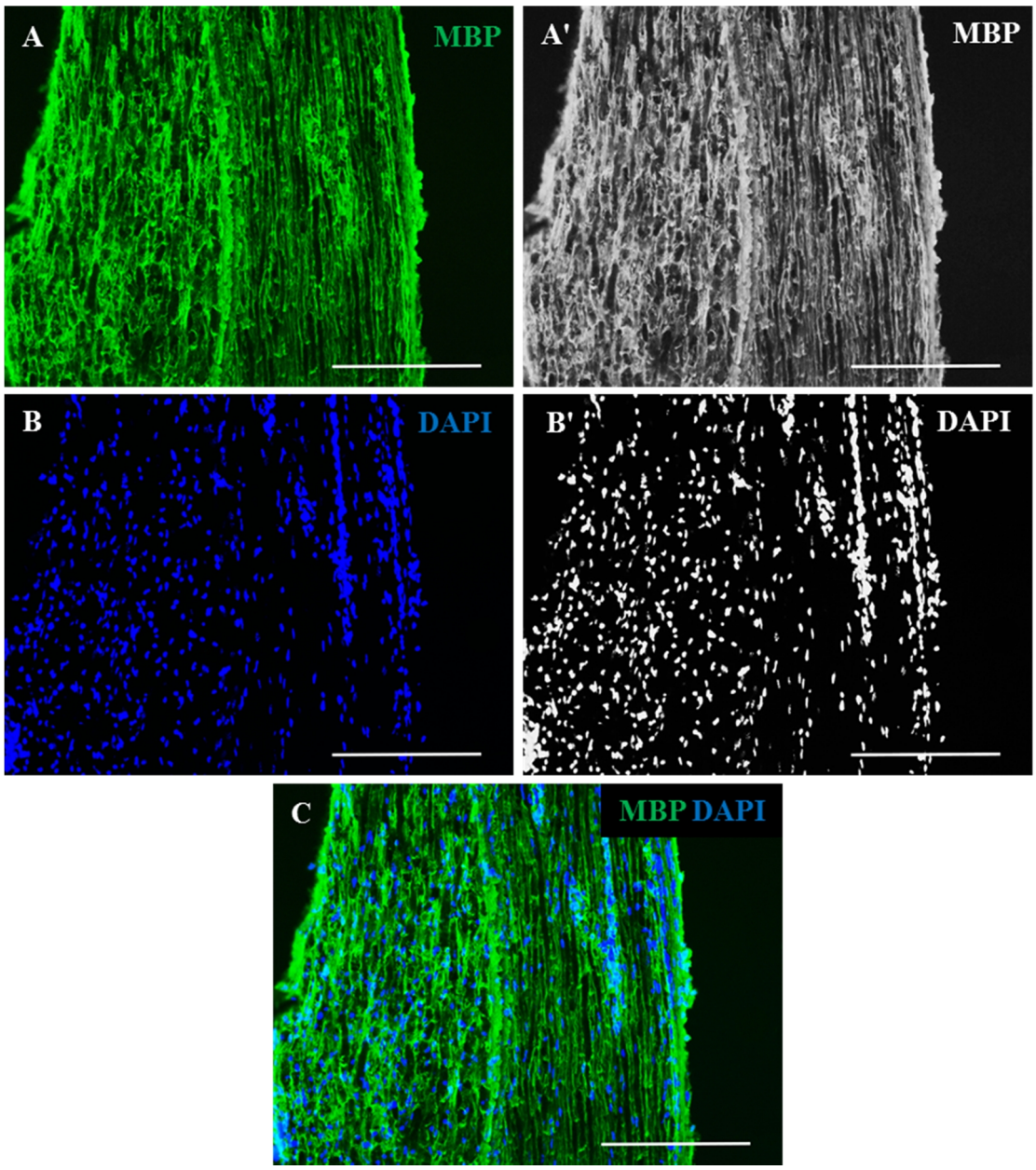

Figure 5.3. Immunolabelling of adult mouse sciatic nerve for MBP (a) that has been injected with 2% of lysolecithin. DAPI staining shows Schwann cell nuclei (b). Merge myelin staining and DAPI is shown in (c). Scale bars represent 100 µm.

5.2. Remyelination Starts Approximately Seven Days After LPC Injection

In order to define the start of remyelination after demyelination, sciatic nerves were investigated in terms of expression using western blots at different time points after lysolecithin (LPC) injection. Nerves were dissected at 1, 7, 14 and 21 days after the injection and used for western analysis of MBP and MAG. MAG is known to be an early myelination marker whereas MBP is a late myelination marker.

The results from this experiment are shown in Figure 5.4 and Figure 5.5. Saline injected nerve was used as a negative control and both sciatic nerves were dissected 1 day after injection. MBP and MAG protein levels were normalized to actin and the difference between three experimental repeats were statistically analyzed.

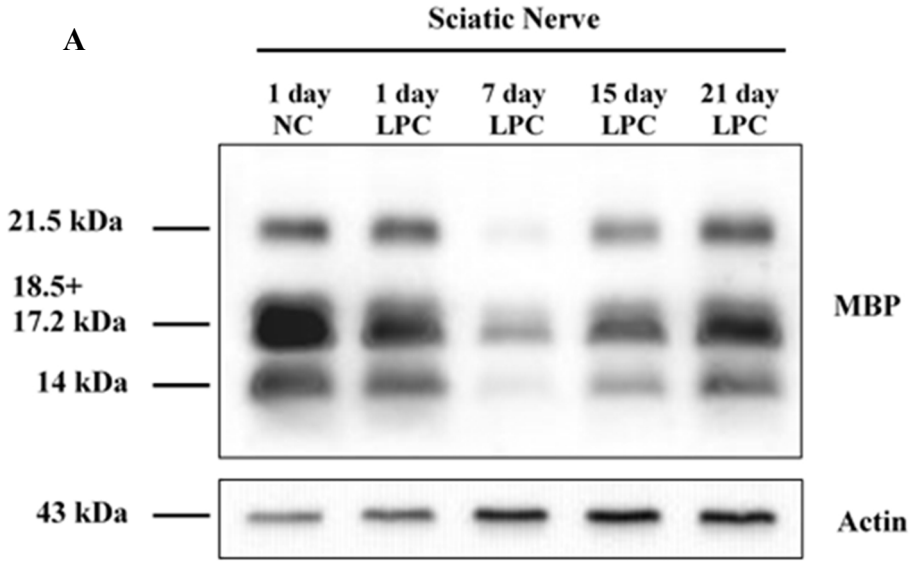

Figure 5.4. Western blotting of MBP after 1, 7, 15 and 21 days from LPC injection. (a) Immunoblotting of MBP. (b) MBP protein level relative to actin level. * $p<0.05$; ** $p<0.01$ (Student T-test method was used to analyze the data). Y-error bars represent SD.

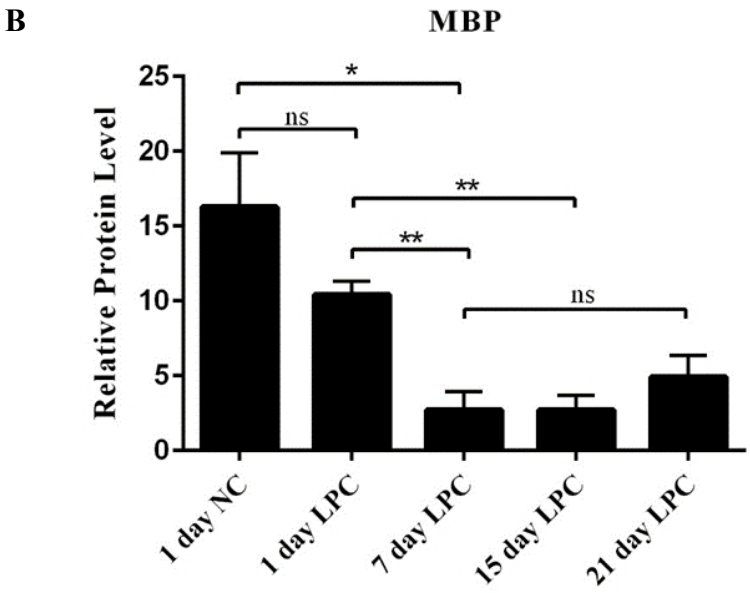

Figure 5.4. Western blotting of MBP after 1, 7, 15 and 21 days from LPC injection. (a) Immunoblotting of MBP. (b) MBP protein level relative to actin level. * $p<0.05$; ** $p<0.01$ (Student T-test method was used to analyze the data). Y-error bars represent SD. (cont.)

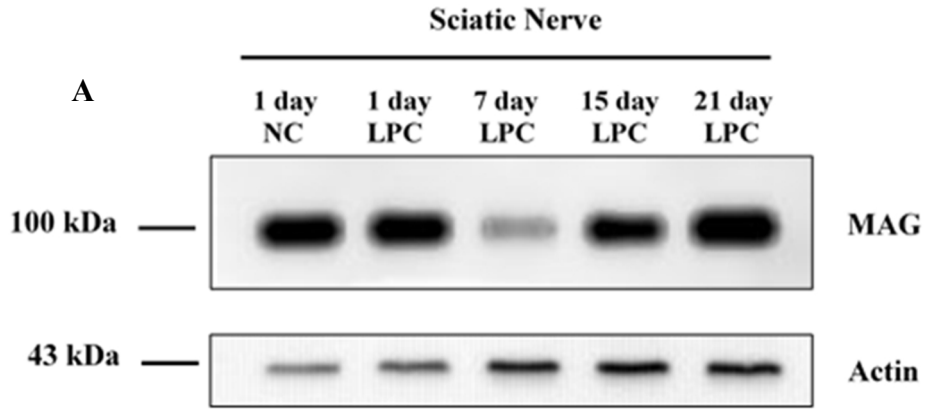

Figure 5.5. Western blotting of MAG after 1, 7, 15 and 21 days from LPC injection. (a) Immunoblotting of MAG. (b) MAG protein level relative to actin level. * $p<0.05$; ** $p<0.01$; *** $p<0.001$ (One-way ANOVA was used to analyze the data). Y-error bars represent SD.

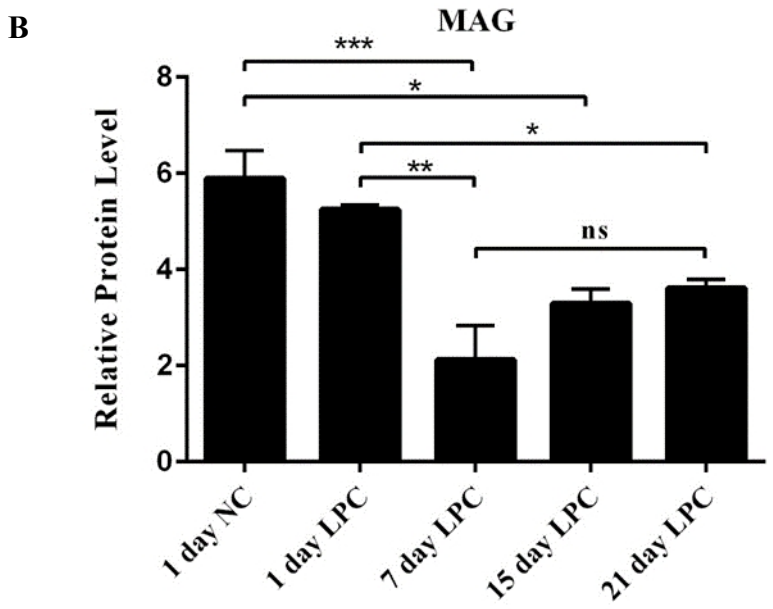

Figure 5.5. Western blotting of MAG after 1, 7, 15 and 21 days from LPC injection. (a) Immunoblotting of MAG. (b) MAG protein level relative to actin level. * $p<0.05$; ** $p<0.01$; *** $p<0.001$ (One-way ANOVA was used to analyze the data). Y-error bars represent SD (cont.)

As seen in Figure 5.4 and Figure 5.5, sciatic nerves dissected 1 and 7 days after lysolecithin injection had clearly decreased MBP and MAG expression compared to negative control, especially at day 7. At day 7, the levels of MBP and MAG decreased to the lowest level, which were then upregulated. These findings suggest that demyelination started with lysolecithin injection and continued until day 7. Since MBP and MAG expression started to increase after day 7 and did not reach the level of negative control until day 21, it can be concluded that remyelination was starting after day 7 and was not completed until day 21.

5.3. Schwann Cell Number is Increased During Remyelination

To see structural changes in myelin sheath during remyelination and also to understand this process in more detail sciatic nerves dissected at 7, 14 and 28 days after lysolecithin injection were immunostained for MBP and NF.

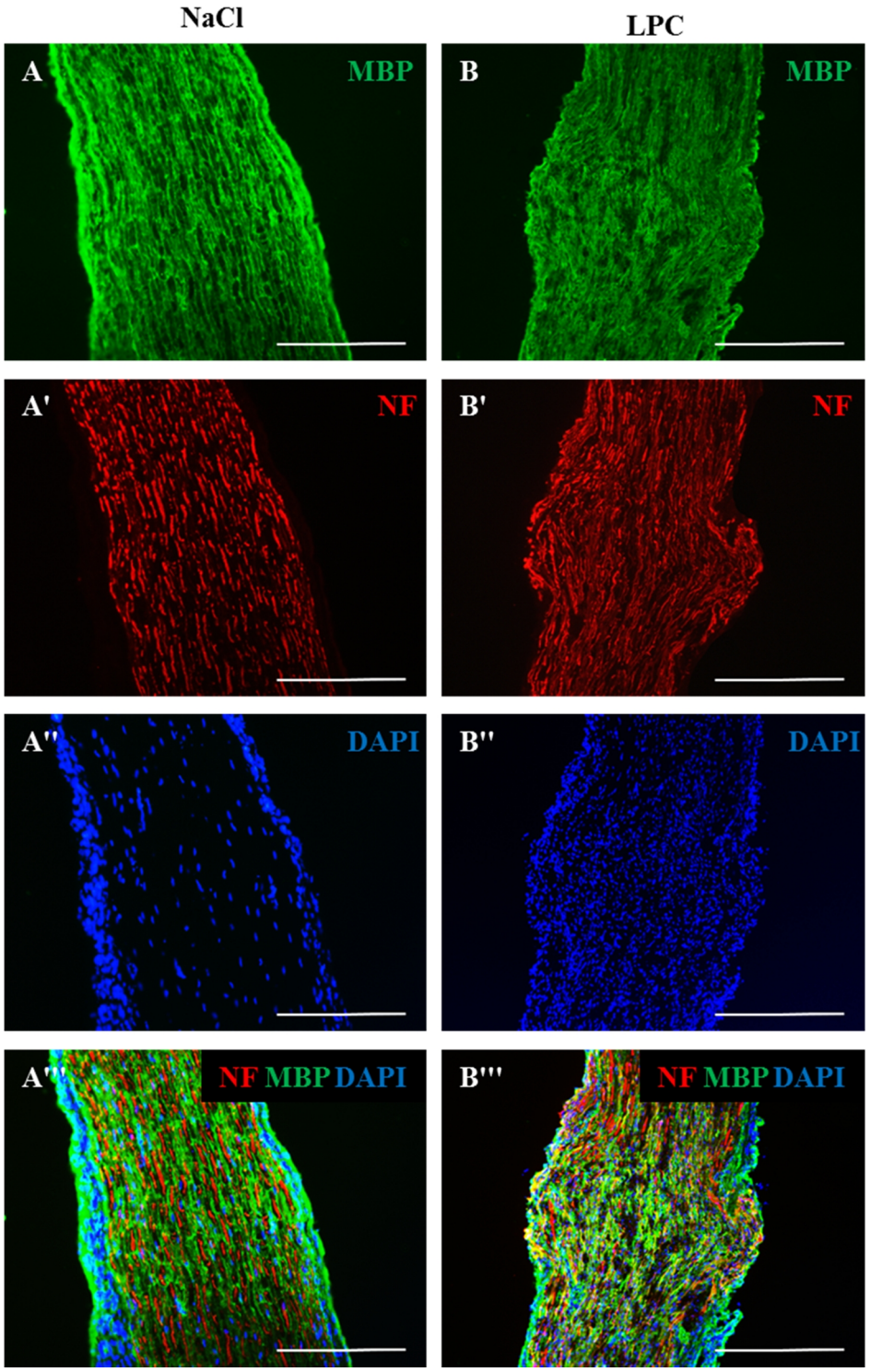

Figure 5.6. Immunolabelling of adult mouse sciatic nerve for MBP and NF dissected 7 days after lysolecithin injection. (a) Saline injected sciatic nerve. (b) Lysolecithin injected sciatic nerve. Scale bars: 200 µm. (c) Number of nuclei in saline and LPC injected nerve. *** $p<0.001$ (Student's t-test was used to analyze the data). Y-error bars represent SEM.

C

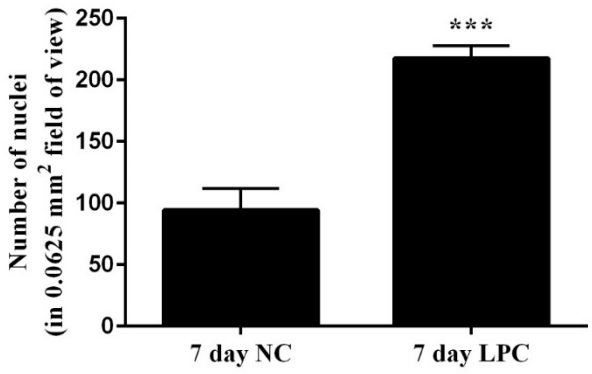

Figure 5.6. Immunolabelling of adult mouse sciatic nerve for MBP and NF dissected 7 days after lysolecithin injection. (a) Saline injected sciatic nerve. (b) Lysolecithin injected sciatic nerve. Scale bars: 200 μm. (c) Number of nuclei in saline and LPC injected nerve. *** $p<0.001$ (Student's t-test was used to analyze the data). Y-error bars represent SEM. (cont.)

Immunolabelling of sciatic nerve dissected 7 days after lysolecithin injection is shown on Figure 5.6 NaCl injected nerve was used as a negative control. In contrast to negative control, myelin sheath in lysolecithin injected nerve had lost its fibrillary structure. Aside from deformation in myelin sheath, axonal deformation was also observable in lysolecithin injected nerve.

Using the immunostainings, number of nuclei, which was stained with DAPI, was counted in 0.0625 mm^2 field of view for both negative control and lysolecithin. Three different regions were counted for each repeat. The increase in the number of nuclei was statistically significant compared to that of the normal tissue. Thus, in addition to structural changes, lysolecithin injected nerve had an increased number of nuclei that could belong to Schwann cells, satellite cells or macrophages.

At day 14, as seen on Figure 5.7, there was again no fibrillary structure in lysolecithin injected nerve, instead myelin sheath seemed as if it was newly formed. As for day 7, the number of nuclei was still significantly high at day 14 compared to negative control.

Figure 5.8 shows immunolabelling of sciatic nerves dissected 28 days after lysolecithin injection. At day 28, number of nuclei decreased to that of day 7. Myelin sheath was seen to recover its fibrillary structure, not completely but partially.

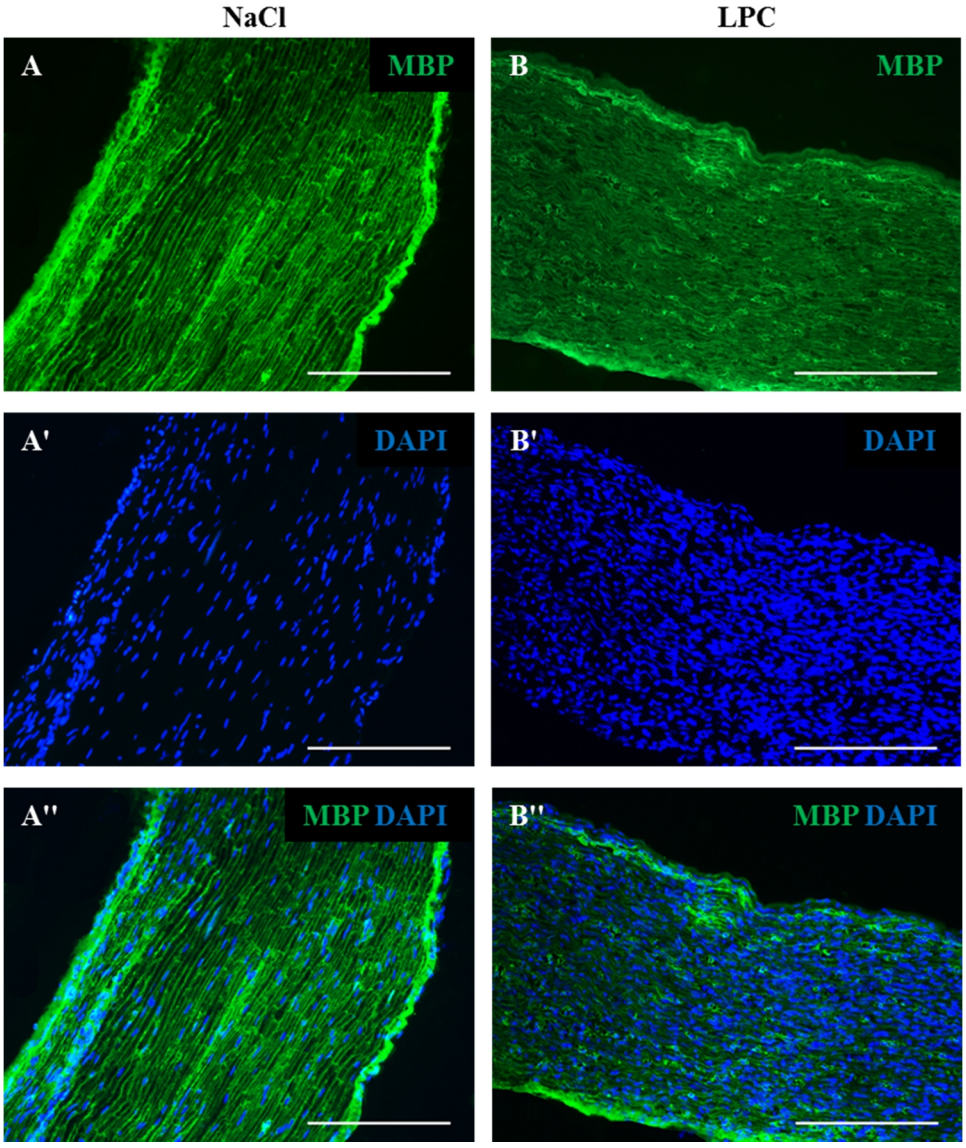

Figure 5.7. Immunolabelling of adult mouse sciatic nerve for MBP dissected 14 days after lysolecithin injection. (a) Saline injected sciatic nerve. (b) Lysolecithin injected sciatic nerve. Scale bars: 200 µm. (c) Numbers of nuclei in saline and LPC injected nerve. **** $p<0.0001$ (Student's t-test was used to analyze the data). Y-error bars represent SEM.

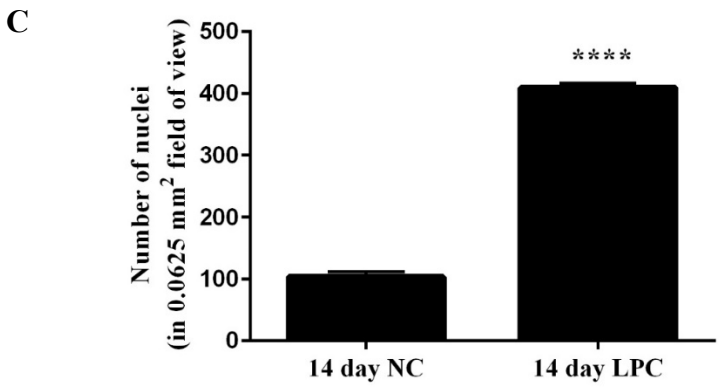

Figure 5.7. Immunolabelling of adult mouse sciatic nerve dissected 14 day after lysolecithin injection for MBP. (a) Saline injected sciatic nerve. (b) Lysolecithin injected sciatic nerve. Scale bars: 200 µm. (c) Numbers of nuclei in saline and LPC injected nerve. **** p<0.0001 (Student's t-test was used to analyze the data). Y-error bars represent SEM. (cont.)

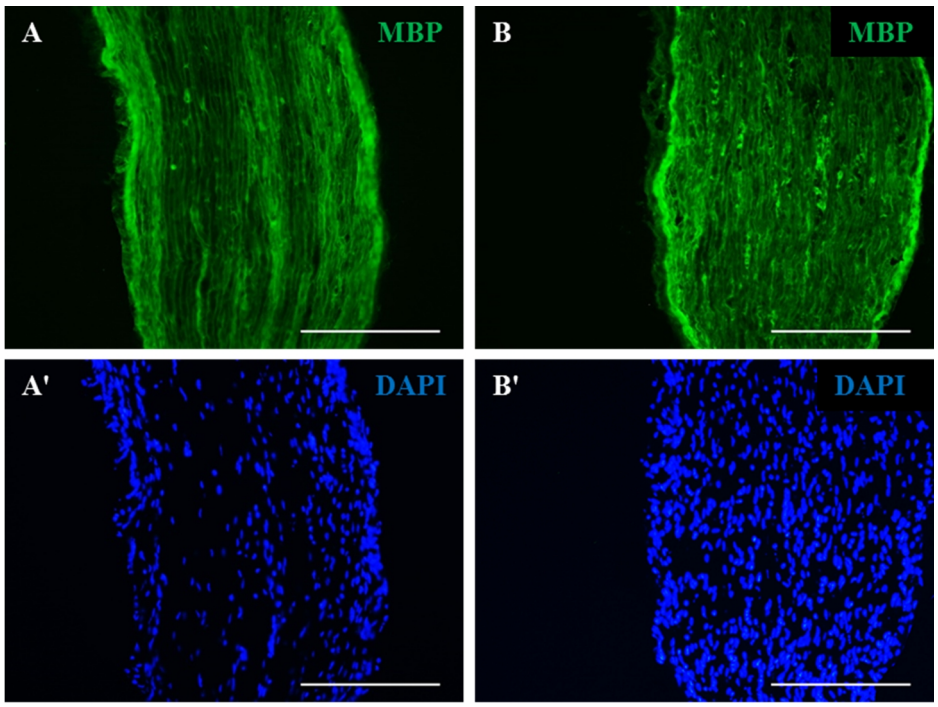

Figure 5.8. Immunolabelling of adult mouse sciatic nerve dissected 28 day after lysolecithin injection for MBP. (a) Saline injected sciatic nerve. (b) Lysolecithin injected sciatic nerve. Scale bars: 200 µm. (c) Numbers of nuclei in saline and LPC injected nerve. * p<0.05 (Student's t-test was used to analyze the data). Y-error bars represent SEM.

C

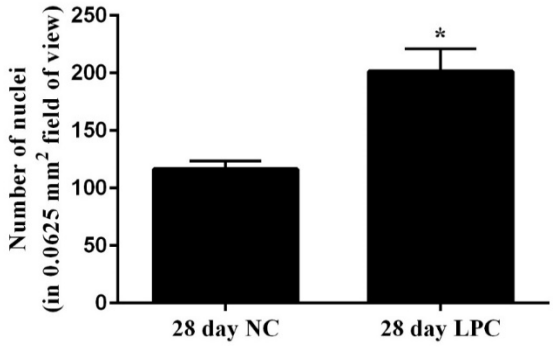

Figure 5.8. Immunolabelling of adult mouse sciatic nerve dissected 28 day after lysolecithin injection for MBP. (a) Saline injected sciatic nerve. (b) Lysolecithin injected sciatic nerve. Scale bars: 200 μm. (c) Numbers of nuclei in saline and LPC injected nerve. * p<0.05 (Student's t-test was used to analyze the data). Y-error bars represent SEM. (cont.)

Changes in nuclei number at days seven, 14 and 28 after lysolecithin injection are shown in the graph on Figure 5.9. As seen, number of nuclei was higher at all time points of lysolecithin injection compared to the negative control. It reaches to its highest level at day 14, and was downregulated at day 28. The number at seven days was similar to the level at day 28.

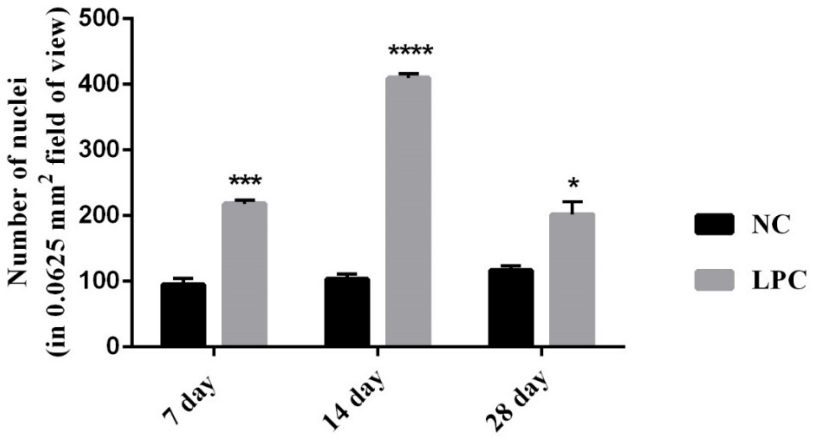

Figure 5.9. Number of nuclei in immunolabelling of adult mouse sciatic nerve dissected seven, 14 and 28 days after lysolecithin injection. * p<0.05; ***p<0.001; ****p<0.0001 (Student's t-test was used to analyze the data). Y-error bars represent SEM.

5.4. FGF1 Level is Upregulated during Remyelination

To see whether if FGF1 level was changing or not during demyelination-remyelination period, mice were sacrificed at 1, 7, 15 and 21 days after lysolecithin injection. Their sciatic nerves were dissected and used for Western analysis of FGF1 and FGF2.

As seen in Figure 5.10, the results showed that seven days after lysolecithin injection, where demyelination was at its highest level, FGF1 was significantly lowered, whereas FGF2 level reached a peak. After day 7, from where remyelination was starting, FGF1 expression was observed to be upregulated, whereas FGF2 expression was down regulated and decreased to a lower level at day 21. The differential regulation of FGF1 and FGF2 observed in our studies are in accordance with the response after demyelinating lesions in the central nervous system (CNS).

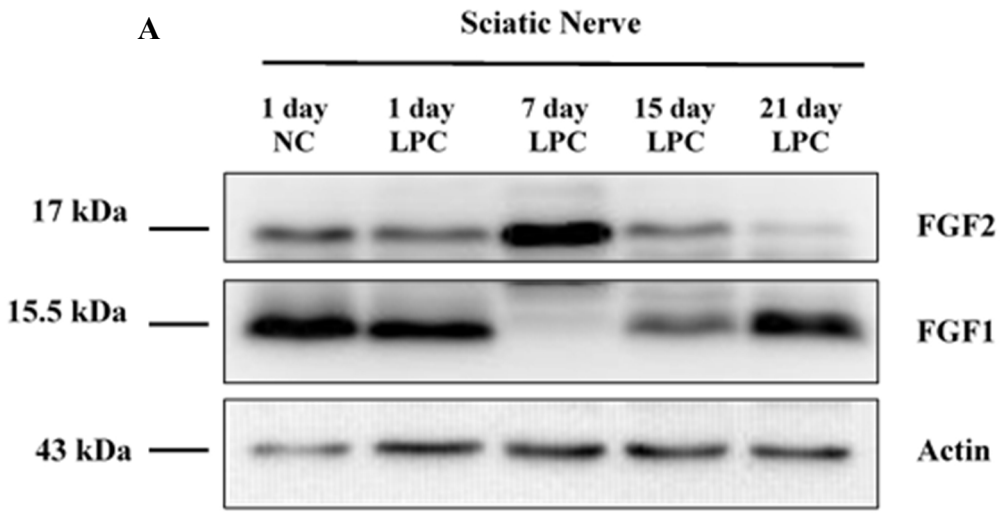

Figure 5.10. Western blotting of FGF1 and FGF2 after 1, 7, 15 and 21 day from LPC injection. (a) Immunoblotting of FGF1 and FGF2. (b) FGF1 protein level relative to actin level. * $p<0.05$; ** $p<0.01$ (Student t-test was used to analyze the data). Y-error bars represent SD.

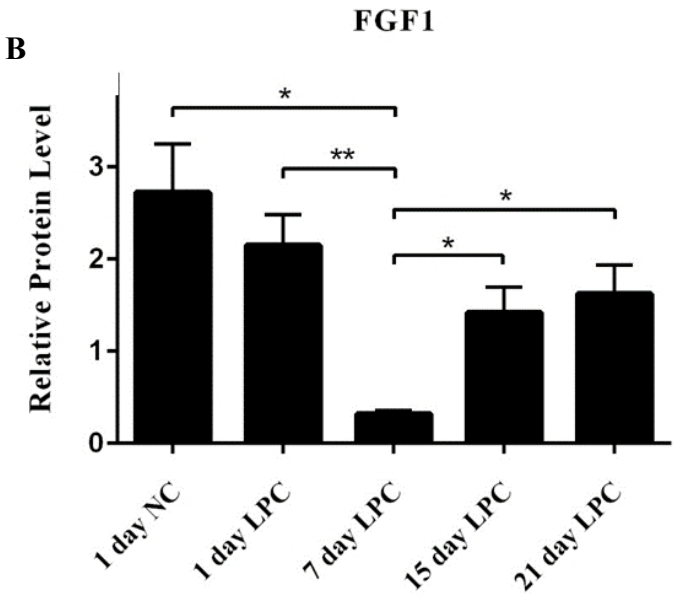

Figure 5.10. Western blotting of FGF1 and FGF2 after 1, 7, 15 and 21 day from LPC injection. (a) Immunoblotting of FGF1 and FGF2. (b) FGF1 protein level relative to actin level. * $p<0.05$; ** $p<0.01$ (Student t-test was used to analyze the data). Y-error bars represent SD. (cont.)

5.5. Blocking of FGF1 Cause Reduction in Remyelination

5.5.1. 20 µg/ml of FGF1 Neutralizing Antibody (Ab9588) Efficiently Blocks FGF1 *in vivo*

The first step was to determine the concentration of the anti-FGF1 neutralizing antibody to be used in blocking reactions. Two different concentrations, 10 µg/ml and 20 µg/ml of the neutralizing agent were used for injections based on the concentrations used in DRG culture to block FGF1 (Dağlıkoca, 2014).

Rabbit IgG1 was used as a control. Right sciatic nerve of mouse was used for anti-FGF1 neutralizing antibody injection, whereas left sciatic of it was used for Rabbit IgG1 injection. 1-2 hour after injection, sciatic nerves were dissected and used for Western analysis of p-FGFR. We were expecting to see a decrease in the phosphorylation level of FGFR, if FGF1 was blocked efficiently. As seen in Figure 5.11, 10 µg/ml of anti-FGF1

neutralizing antibody did not cause a difference in phosphorylation level of FGFRs, while 20 µg/ml of the antibody was shown to decrease the level of p-FGFR.

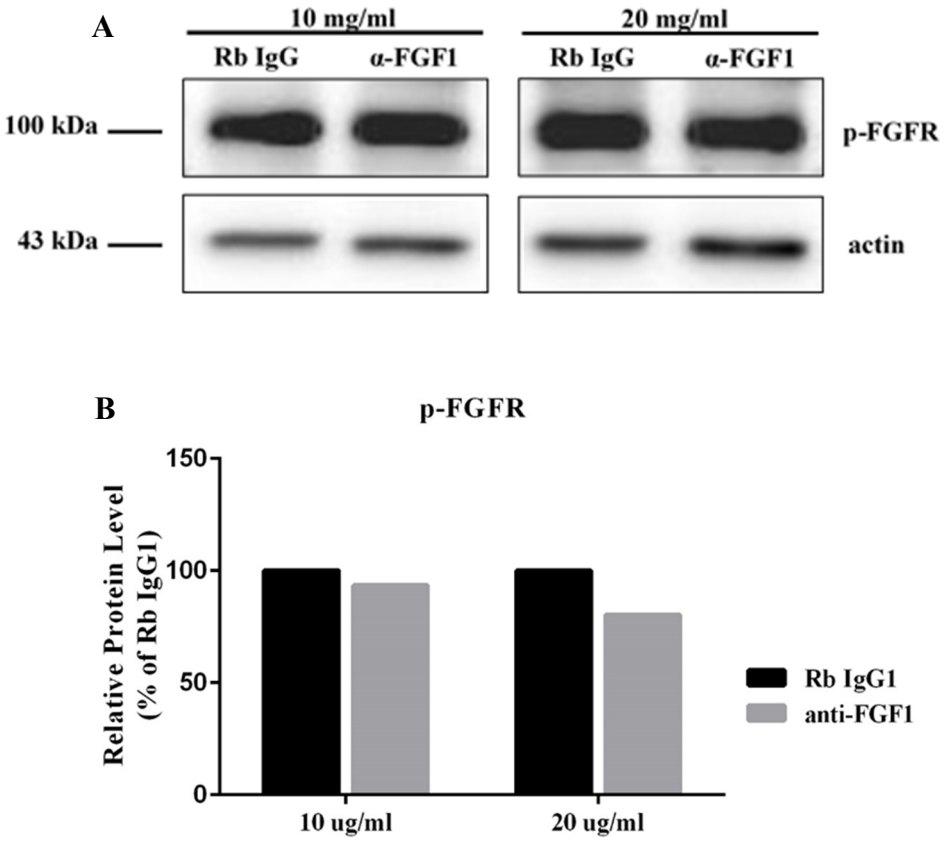

Figure 5.11. Western blotting of p-FGFR after 10 and 20 µg/ml anti-FGF1 neutralizing antibody injection. (a) Immunoblotting of p-FGFR. (b) p-FGFR protein level relative to actin level.

The experiment was repeated for 20 µg/ml of anti-FGF1 neutralizing antibody, but this time we increased the volume of the injected solution to enlarge the area that the blocker can diffuse. As seen in Figure 5.12, p-FGFR level significantly decreased after injection of 20 µg/ml anti-FGF1 neutralizing antibody.

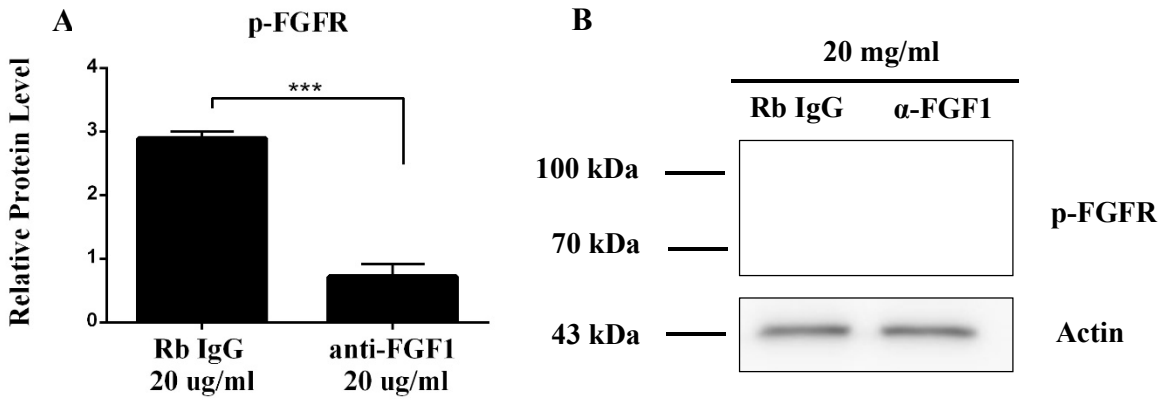

Figure 5.12. Western blotting of p-FGFR 20 µg/ml anti-FGF1 neutralizing antibody injection. (a) p-FGFR protein level relative to actin level. *** $p<0.001$ (Student t-test was used to analyze the data). Y-error bars represent SEM. (b) Immunoblotting of p-FGFR after 20 µg/ml anti-FGF1 neutralizing antibody injection.

5.5.2. Blocking of FGF1 During Remyelination Causes a Decrease in MBP and MAG Expression

In order to investigate the role of FGF1 during remyelination period, sciatic nerves were injected with lysolecithin to induce demyelination, and then were injected with either FGF1 neutralizing antibody (Ab9588) or Rabbit IgG1 (for negative control injections) 8 days later, and again 12 days later, at a time when Schwann cells actively remyelinate in the lesion. After 14 days from initial lysolecithin injection, nerves were dissected and used for Western blot analysis of MBP and MAG.

Figure 5.13 shows western blot results of MAG, which is an early myelin marker. MAG expression was seen to be downregulated as a consequence of FGF1 blocking. As seen in Figure 5.14, level of MBP, which is a late myelin marker, also significantly decreased after FGF1 neutralizing antibody injection compared to that of Rabbit IgG1 injected ones. Since expression of early and late myelin markers, MAG and MBP respectively, decreased when FGF1 was blocked during remyelination, it can be suggested that FGF1 might have a role in the remyelination period.

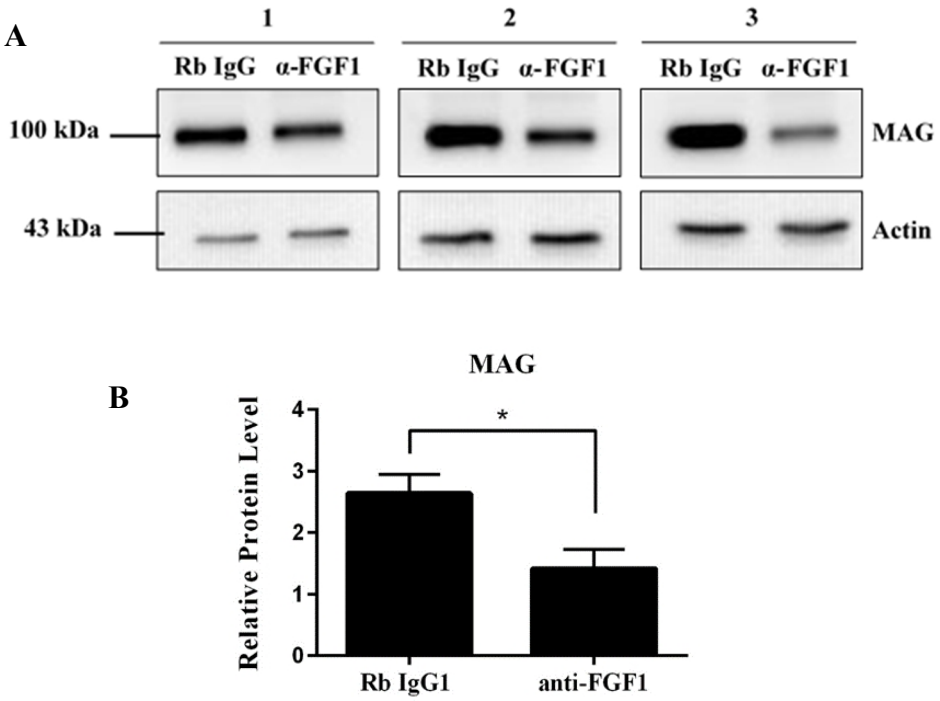

Figure 5.13. Western blotting of MAG after two repetitive injections of anti-FGF1 blocking antibody following demyelination. (a) Immunoblotting of MAG. 1, 2 and 3 are experimental repeats. (b) MAG protein level relative to actin level. * $p<0.05$ (Student t-test was used to analyze the data). Y-error bars represent SD.

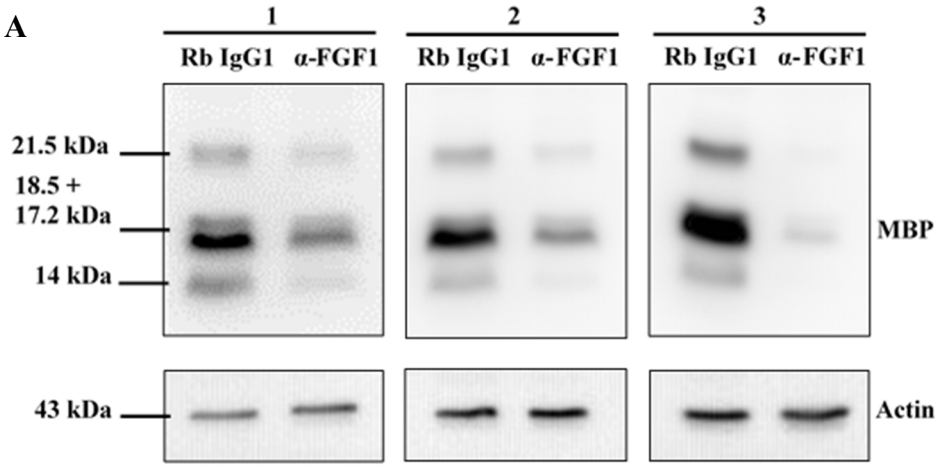

Figure 5.14. Western blotting of MBP after two times injection of anti-FGF1 blocking antibody following demyelination. (a) Immunoblotting of MBP. 1, 2 and 3 are experimental repeats. (b) MBP protein level relative to actin level. * $p<0.05$ (Student t-test was used to analyze the data). Y-error bars represent SD.

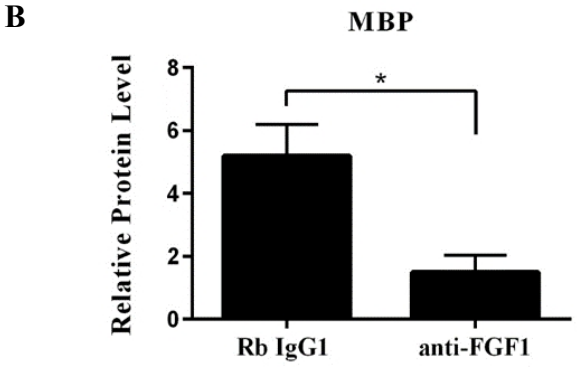

Figure 5.14. Western blotting of MBP after two repetitive injections of anti-FGF1 blocking antibody following demyelination. (a) Immunoblotting of MBP. 1, 2 and 3 are experimental repeats. (b) MBP protein level relative to actin level. * $p<0.05$ (Student t-test was used to analyze the data). Y-error bars represent SD. (cont.)

5.6. Blocking of FGFR1, FGFR2 or FGFR3 Has No Significant Effect on Remyelination

In order to find through which receptor FGF1 acts during remyelination, FGFR1, FGFR2 and FGFR3 were separately inhibited during remyelination by using neutralizing antibodies, which are MAB765, MAB684 and MAB710, respectively. After 8 and 12 days from initial lysolecithin injection, sciatic nerves were injected either with FGFR1/2/3 neutralizing antibody or control IgG (for negative control injections). Finally, after 14 days from initial lysolecithin injection, they were dissected and used for Western blot analysis.

5.6.1. FGFR1 Blocking

FGFR1 was blocked by using anti-FGFR1 blocking antibody (R&D, MAB765) during active remyelination period. Hundred μg/ml of anti-FGFR1 neutralizing antibody was used for blocking injections. In order to investigate the effect of FGFR1 block on myelination, sciatic nerves were dissected 14 days after initial lysolecithin injection and used for expression analysis of MAG and MBP.

Figure 5.15 shows the change in MBP expression after FGFR1 inhibition during remyelination. Mouse IgG1 was used for negative control injections instead of anti-FGFR1

neutralizing antibody. After FGFR1 blocking, MBP expression increased compared to negative control, but the increase was not statistically significant.

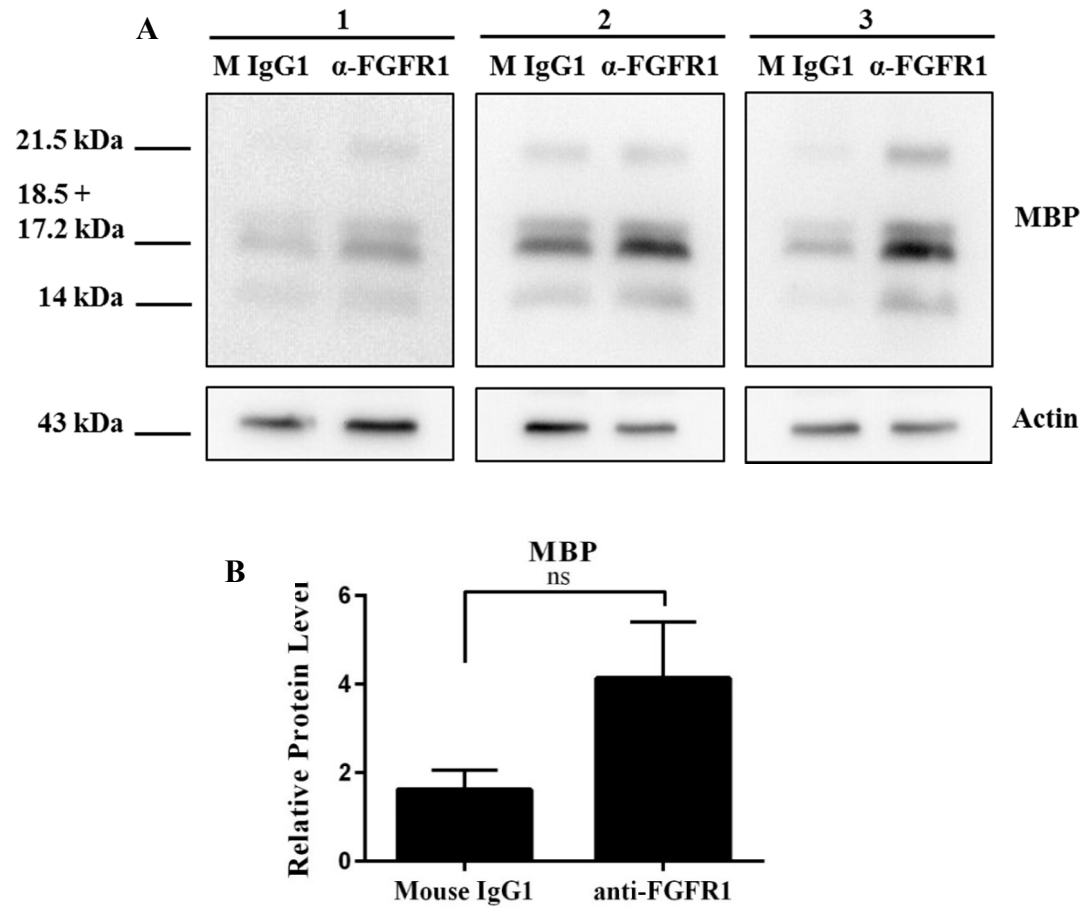

Figure 5.15. Western blotting of MBP after two repetitive injections of anti-FGFR1 blocking antibody following demyelination. (a) Immunoblotting of MBP. 1, 2 and 3 are experimental repeats. (b) MBP protein level relative to actin level. ns = not significant (Student t-test was used to analyze the data). Y-error bars represent SD.

MAG expression after two times anti-FGFR1 neutralizing antibody injection following 2% lysolecithin injection is shown on Figure 5.16. Similar to MBP, MAG expression also increased to a certain level when FGFR1 was blocked during remyelination. The increase in MAG expression was again not statistically significant.

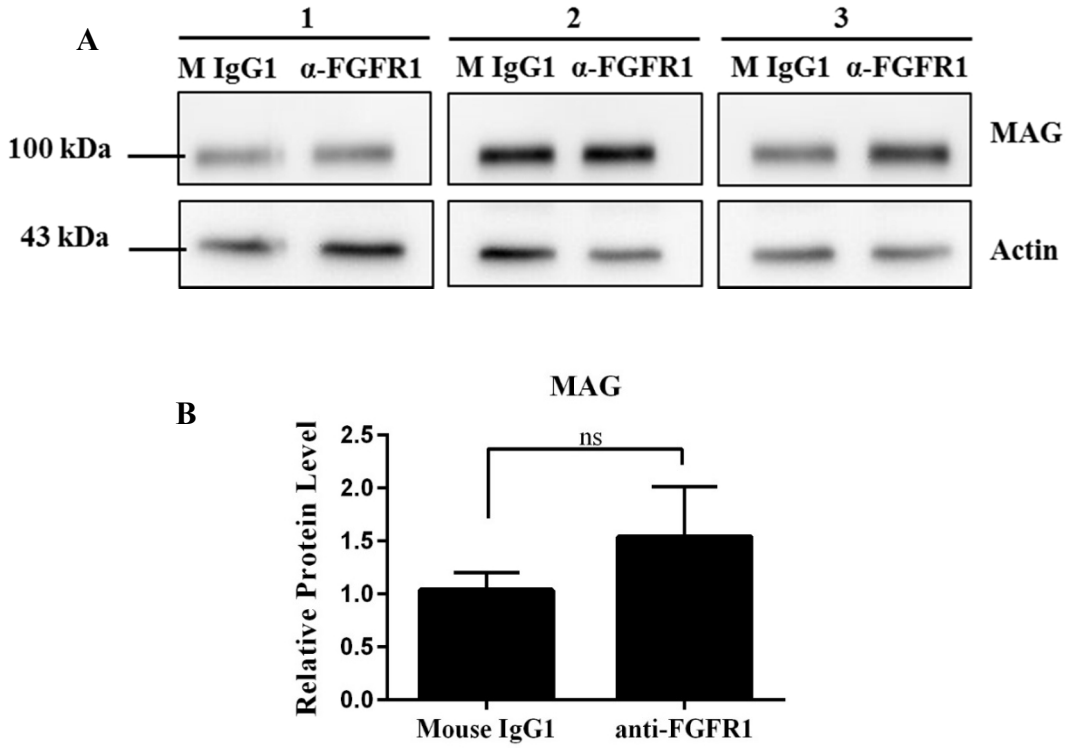

Figure 5.16. Western blotting of MAG after two repetitive injections of anti-FGFR1 blocking antibody following demyelination. (a) Immunoblotting of MAG. 1, 2 and 3 are experimental repeats. (b) MAG protein level relative to actin level. ns = not significant (Student t-test was used to analyze the data). Y-error bars represent SD.

5.6.1.1. Signaling pathway activated by FGFR1 during remyelination. Our study has demonstrated that FGFR1 can have a role during remyelination In order to further understand its role in remyelination, signaling pathway activated by it should be known. Therefore, p-AKT, p-ERK ½ and p-PLC gamma 1 expression were analyzed in FGFR1 blocked sciatic nerve by using Western blot analysis.

Western blotting results are shown on Figure 5.17. After normalization of all proteins to actin, p-ERK/ERK, p-AKT/AKT and p-PLC gamma 1/PLC gamma 1 ratios were calculated. As seen on Figure 5.17., p-ERK level increased, when FGFR1 was blocked. This increase was again statistically not significant as the increase in MAG and MBP expression. p-AKT and p-PLC gamma 1 levels, on the other hand, did not change in comparison to negative control.

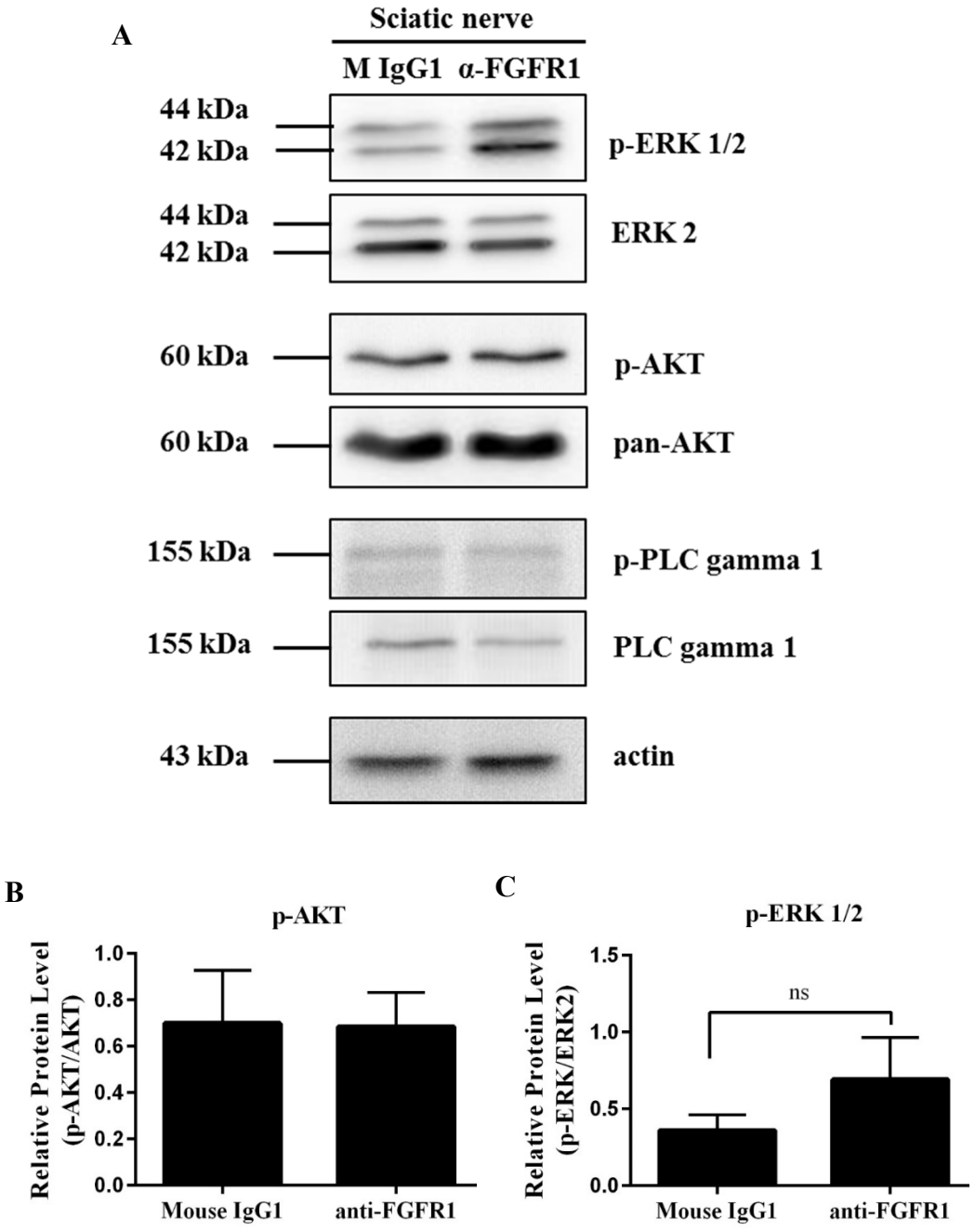

Figure 5.17. Western blotting of p-ERK1/2, p-AKT and p-PLC gamma 1 after two repetitive injections of anti-FGFR1 blocking antibody. (a) Immunoblotting of p-ERK1/2/ERK2, p-AKT/AKT and p-PLC gamma 1/PLC gamma 1. (b) p-AKT, (c) p-ERK 1/2 and (d) p-PLC gamma 1 levels relative to actin levels. ns=not significant. Student t-test was used for statistical analysis. Y-error bars represent SD.

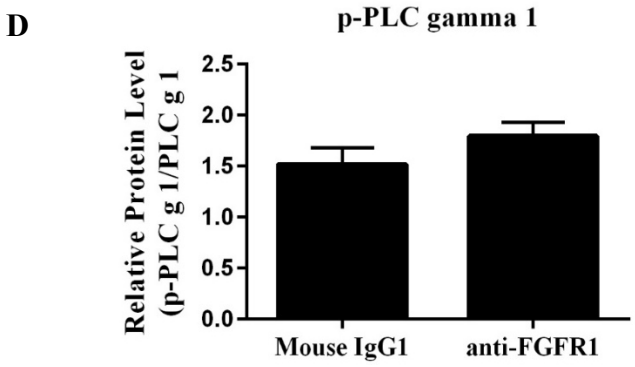

Figure 5.17. Western blotting of p-ERK1/2, p-AKT and p-PLC gamma 1 after two repetitive injection of anti-FGFR1 blocking antibody. (a) Immunoblotting of p-ERK1/2/ERK2, p-AKT/AKT and p-PLC gamma 1/PLC gamma 1. (b) p-AKT, (c) p-ERK 1/2 and (d) p-PLC gamma 1 levels relative to actin levels. ns=not significant. Student t-test was used for statistical analysis. Y-error bars represent SD. (cont.)

5.6.2. FGFR2 Blocking

To investigate the possible role of FGFR2 in the remyelination process, FGFR2 was blocked by using anti-FGFR2 neutralizing antibody (R&D, MAB684) during active remyelination period. Hundred µg/ml of anti-FGFR2 neutralizing antibody was used for blocking injections. The effect of FGFR2 blocking on remyelination was investigated by Western blotting for MBP and MAG after 14 days from initial lysolecithin injection. Mouse IgG was used for negative control injections.

As seen on Figure 5.18 and Figure 5.19, FGFR2 blocking during remyelination period did not cause a statistically significant difference in MAG and MBP expression compared to negative control.

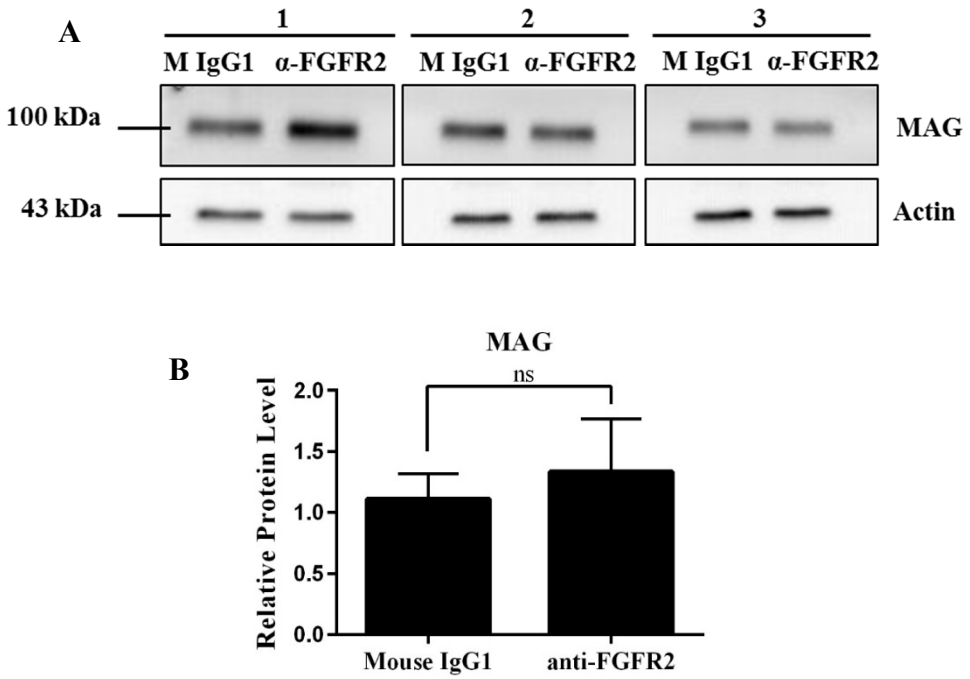

Figure 5.18. Western blotting of MAG after two repetitive injections of anti-FGFR2 neutralizing antibody following demyelination. (a) Immunoblotting of MAG. 1, 2 and 3 are experimental repeats. (b) MAG level relative to actin. ns = not significant (Student's t-test was used for statistical analysis). Y-error bars represent SD.

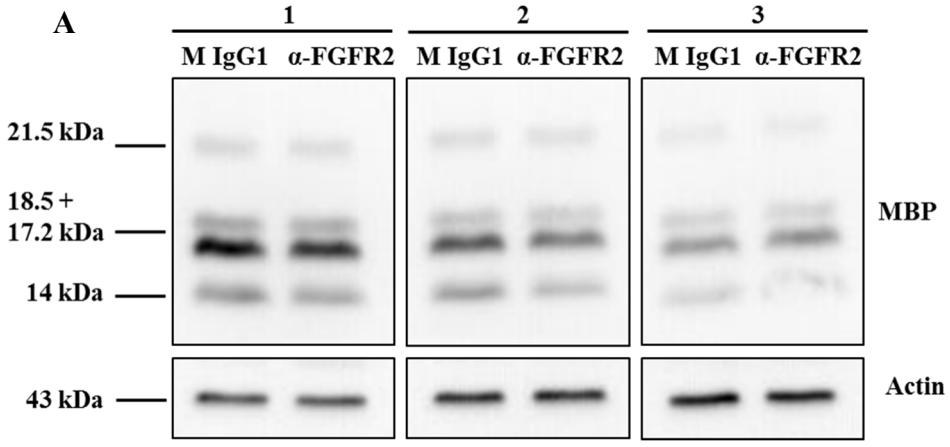

Figure 5.19. Western blotting of MBP after two repetitive injections of anti-FGFR2 neutralizing antibody following demyelination. (a) Immunoblotting of MBP. 1, 2 and 3 are experimental repeats. (b) MBP level relative to actin. ns = not significant (Student's t-test was used for statistical analysis). Y-error bars represent SD.

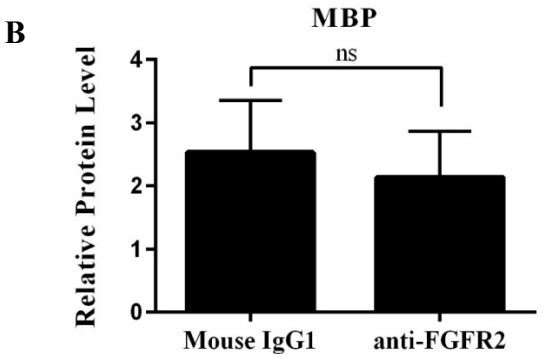

Figure 5.19. Western blotting of MAG after two repetitive injections of anti-FGFR2 neutralizing antibody following demyelination. (a) Immunoblotting of MAG. 1, 2 and 3 are experimental repeats. (b) MAG level relative to actin. ns = not significant (Student's t-test was used for statistical analysis). Y-error bars represent SD. (cont.)

5.6.3. FGFR3 Blocking

The role of FGFR3 in remyelination process was also investigated. The protein activity was blocked by using 200 µg/ml of anti-FGFR3 neutralizing antibody (R&D, MAB710) during active remyelination period. The anti-FGFR3 neutralizing antibody was injected at day 8, and again at day 12, after initial lysolecithin injection. Sciatic nerves were then dissected 14 days after initial lysolecithin injection and used for Western blotting of MAG and MBP. Rat IgG2A was injected as a negative control. Figure 5.20 and Figure 5.21 show MBP and MAG expression after FGFR3 blocking. As seen on figures, when FGFR3 was blocked, MAG and MBP expression was not affected.

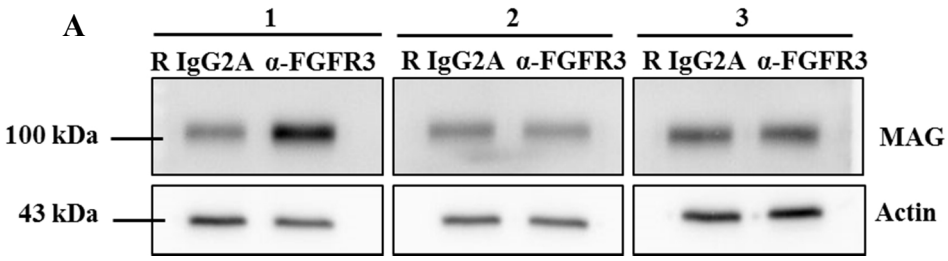

Figure 5.20. Western blotting of (a) MAG and (b) MBP after two repetitive injections of anti-FGFR3 neutralizing antibody following demyelination. 1, 2 and 3 are experimental repeats.

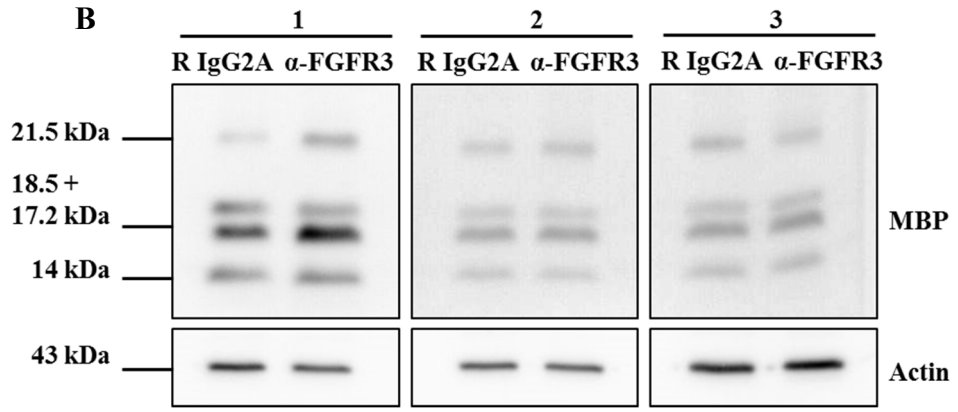

Figure 5.20. Western blotting of (a) MAG and (b) MBP after two repetitive injections of anti-FGFR3 neutralizing antibody following demyelination. 1, 2 and 3 are experimental repeats. (cont.)

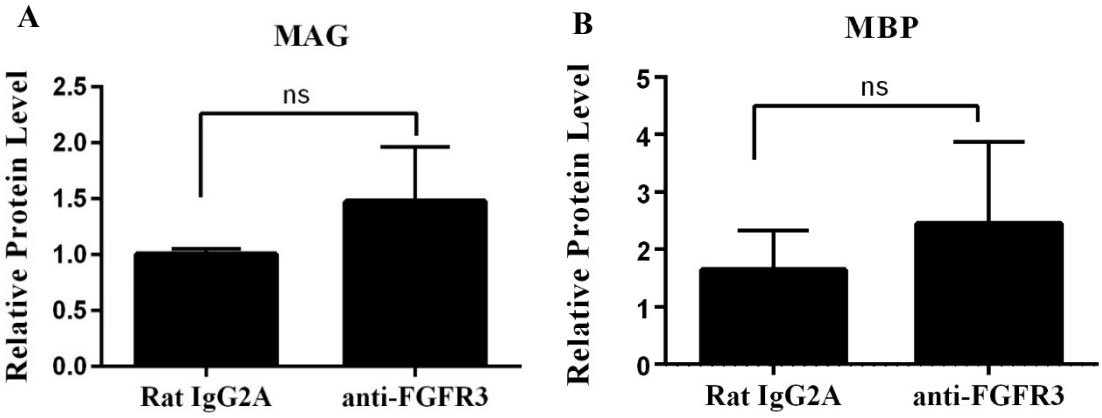

Figure 5.21. (a) MAG and (b) MBP protein levels relative to actin after two repetitive injections of anti-FGFR3 neutralizing antibody following demyelination. ns = not significant (Student's t-test was used for statistical analysis). Y-error bars represent SD.

5.7. FGF1 Blocking Did Not Affect Phosphorylation of FGFR1, FGFR2 and FGFR3

In order to see whether phosphorylation level of FGFRs changed when FGF1 is blocked, immunoprecipitation assays were performed. FGFR1, FGFR2 and FGFR3 were precipitated separately and then were used for Western blotting of p-FGFR. We expected to observe a decrease in phosphorylation level of the receptor, if FGF1 acts through FGFRs during remyelination.

As seen on Figure 5.22, there was no difference in phosphorylation levels of FGFR1 (Figure 5.22a), FGFR2 (Figure 5.22b) and FGFR3 (Figure 5.22c) compared to their levels in negative controls.

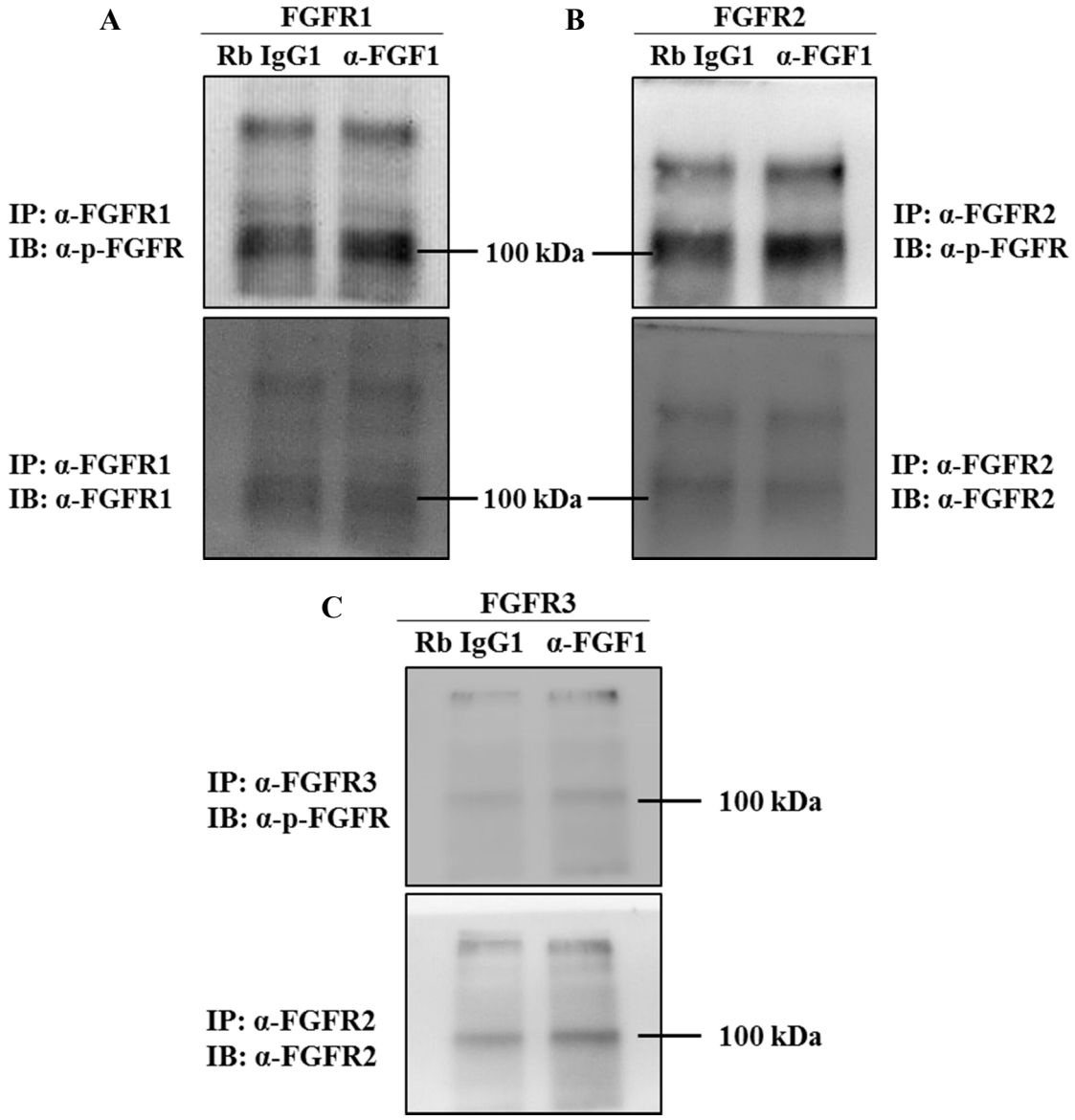

Figure 5.22. Immunoblotting of immunoprecipitated FGFR1 (a), FGFR2 (b) and FGFR3 (c) for p-FGFR after FGF1 blocking.

6. DISCUSSION

The major cellular components of the PNS, axon and Schwan cell, are in a continuous bi-directional communication both during development and adulthood [2]. Axon derived signals regulate the proliferation and differentiation of Schwann cells [18], whereas Schwann cells determine the axonal architecture and support the maintenance and survival of the axons. Disruption of this highly regulated interaction is the main reason of Charcot-Marie Tooth (CMT) also known as Hereditary Motor and Sensory Neuropathies (HMSN). It is a heterogeneous group of inherited disorders affecting both motor and sensory nerves [57]. Understanding the molecular mechanism of this interaction is important to shed light on the pathology of CMT [58]. The most well-known protein that has been shown to act in this interaction is NRG1. It is secreted from axons and regulates Schwann cell differentiation, proliferation, migration and survival as well as regeneration through ErbB2/3 receptors located in Schwann cell membrane [23, 59-62]. Previous studies performed in our laboratory (Dağlıkoca, 2014) demonstrated that the localization pattern of FGF1 is similar to that of NRG1. Furthermore, it was shown that FGF1 may have a possible role during peripheral nervous system myelination. Thus, in this study, we aimed to further investigate the possible role of FGF1 and its receptors (FGFR1-3) during peripheral nerve myelination through *in vivo* experiments.

To accomplish our aim, initially, we made a literature search for *in vivo* studies of the PNS and determined to use PNS remyelination procedure. In this experimental procedure, lysolecithin injection into the nerve results in demyelination that is followed by a remyelination period and this period is fundamentally similar to developmental myelination. By using this model, various substances can be examined for their effect on myelination by directly injecting into the nerve after lysolecithin-induced demyelination. Furthermore, it allows to work with adult mice instead of newborn and, thus, prevents technical problems emerging while working with newborn mice with thin nerves [63].

In the first part of the study, we investigated whether we could induce a demyelinating lesion by lysolecithin injection into mouse sciatic nerve and determined the dose of the molecule. The results showed that 1% of lysolecithin induces demyelination but

it is restricted only to the injection site (Figure 5.2). To improve the effect of lysolecithin, we increased the concentration to 2%, and the volume of the solution. Contrary to the well-defined, fibrillary-like structure of the saline injected sciatic nerve (Figure 5.1), lysolecithin-injected nerve was shown to lose its fibrillary like structure and the compact myelin was loosened (Figure 5.3). This finding was implicating that we were successful in the implementation of the PNS remyelination procedure. The observed distortions in the structure were probably due to induced demyelination and degradation of the proteins present in compact myelin structure, such as PMP22, MPZ and MBP.

To define the time point for the initiation of remyelination, lysolecithin injected nerves that were dissected at different time points (1, 7, 15 and 21 days after lysolecithin injection) were investigated in terms of expression of major myelin proteins, MAG and MBP. Our results showed that the nerves after lysolecithin injection had a clearly decreased MBP and MAG expression compared to saline injected nerve (Figure 5.4 and Figure 5.5). Seven days after lysolecithin injection, the expression of both MAG and MBP decreased to their lowest levels. The data also implicated upregulation of these genes/proteins at the end of the seventh day of injection. It has been known that after a peripheral nerve injury, the disruption of axon-Schwann cell interaction causes Schwann cells to downregulate their myelin specific genes [28]. Therefore, the initial decrease in the level of myelin proteins, MAG and MBP, at 1-day was probably because of the downregulation of their expression due to the initiation of demyelination. During demyelination, Schwann cells initiate the degradation of myelin debris and recruit macrophages to the injury site through inflammatory mediators. Macrophages are responsible for final removal of myelin debris [31]. Thus, it can be suggested that the decrease at seventh day can be a consequence of the degradation of myelin debris by Schwann cells in conjunction with recruited macrophages. The increase in the level of MAG and MBP at 15-day samples could be an indicator of remyelination. Remyelination is known to start seven days after lysolecithin injection in rats [32, 64]. According to our results, it can be concluded that remyelination started at around 7-15 days after lysolecithin injection and these results are in accordance with the previous reports in mice [34].

To examine the structural changes occurring during remyelination period, we used immunohistochemical analysis and investigated the sciatic nerve that were dissected at

seven, 14 and 28 days after lysolecithin injection. At day seven, the myelin sheaths were irregularly oriented with no fibrillary structure probably due to loosening of the Schwann cell folding around the axons (Figure 5.6). Locally demyelinated sites were also observable in the nerve, which would mean that remyelination has not started yet. On the contrary, at day 14, the nerve did not still recover from demyelination effect (Figure 5.7). Finally, at day 28, the myelin sheath partially regained its fibrillary-like structure (Figure 5.8). In the light of molecular and cellular findings we concluded that initiation of remyelination may take place between 7^{th} and 14^{th} days after lysolecithin injection.

The loss of axonal contact occurring as a result of peripheral injuries causes dedifferentiation of myelinating Schwann cell and promotes their proliferation. Two distinct phases of Schwann cell proliferation occurs after peripheral nerve injuries. The first phase of proliferation is seen during demyelination process, while second phase of proliferation take place during the regenerative processes [28]. The injury-induced proliferation of Schwann cells can be responsible for the replacement of dead or dying cells and production of neurotrophic factors to support demyelinated axons [32]. However, recently, it was proposed that proliferation of Schwann cell is not necessarily needed for remyelination of peripheral nerves, since in the absence of Schwann cell proliferation after an injury, remyelination occurs normally in every respect [65]. Thus, Schwann cell proliferation may have a regulatory function during remyelination. In our studies, we also performed DAPI stainings to label cell nuclei and follow the increase in their number to provide further evidence for induction of demyelination in our system. Lysolecithin injected nerves had a higher number of nuclei compared to those injected with saline for all investigated time points (Figure 5.6, 5.7 and 5.8), however the number was highest at 14^{th} day. The increase in nuclei number at day seven can be attributed to both Schwann cell proliferation and macrophage recruitment to demyelinated site. Observation of a higher number at day 14 compared to day seven, may be a consequence of second phase Schwann cell proliferation that occurs during remyelination. At day 28, the number of cell nuclei was decreased, but it was still in high number compared to negative controls. One possible explanation of this decrease can be the apoptosis of the proliferated Schwann cells after remyelination is initiated. Therefore, we can again conclude that our system perfectly worked and we could induce demyelination followed by remyelination by lysolecithin injection.

To unravel the possible role of FGF1 during peripheral nerve myelination, we initially investigated FGF1 expression during demyelination-remyelination period (one, seven, 15 and 21 days after lysolecithin injection). We were expecting to see an increase in its expression, if it had a direct role during remyelination of Schwann cells. Since FGF2 is known to be upregulated after peripheral nerve injuries, we also analyzed it as a control. Our results (Figure 5.10) showed that FGF1 level is downregulated during demyelination, while the expression of FGF2 is significantly upregulated. As expected, together with the initiation of remyelination the expression of FGF1 is upregulated and it reached its original level gradually by day 21. On the contrary, FGF2 was shown to be downregulated during remyelination period. The expected increase in the expression of FGF1 in remyelination period that mimics developmental myelination, further demonstrated the importance of FGF1 for Schwann cell myelination. The increased level of FGF2 during peripheral nerve injuries is thought to promote the proliferation of Schwann cell and inhibit myelination through FGFR1/FGFR2 signaling [52]. Therefore, the upregulation of FGF2 expression in lysolecithin injected sciatic nerve may be an indicator of its involvement in Schwann cell proliferation during demyelination period. According to these results, it can be proposed that both FGF1 and FGF2 are involved in demyelination and remyelination processes, but they may be active in different time points with exactly opposite function.

Antigen-specific blocking antibodies have the ability to precisely inhibit the function of a particular protein and this approach is very efficient when investigating the probable function of a specific protein [66]. Therefore, to inhibit the activity of FGF1 during remyelination of Schwann cells, we preferred to use FGF1 specific neutralizing antibody that was also used by Dağlıkoca (2014) in DRG culture experiments. Our previous experiments had shown that remyelination starts between 7^{th} and 14^{th} days after lysolecithin injection. Taking this finding as a reference, we chose days 8 and 12 for repetitive FGF1 blocking injections FGF1 (Figure 5.13 and Figure 5.14, respectively) Inhibition of FGF1 during remyelination period caused a significant reduction in the level of myelin proteins, MAG and MBP implicating that FGF1 is responsible for the upregulation of myelin specific proteins during remyelination in our experiments. This finding was critical since it was demonstrating the role of FGF1 during normal peripheral nervous system myelination since our system was fundamentally similar to developmental myelination. During remyelination process, FGF1 can be produced by the axons, as previously shown in our laboratory both in

DRG co-culture and adult mouse sciatic nerve, or Schwann cells. If it is produced by the axons, it probably acts trough FGF receptors (FGFR1-3) located on Schwann cell plasma membrane. Because FGF receptors were shown to be present in Schwann cells not on neurons by Dağlıkoca, if FGF1 is produced by Schwann cells, two possibilities arise to exert its action: it can either act through autocrine signaling or in a receptor independent manner.

To examine these possibilities, in the third part of the study, we focused on the inhibition of FGF receptor (FGFR1, FGFR2 and/or FGFR3) separately during remyelination period by injecting blocking antibodies. Similar to FGF1 related experiments, blocking antibody injections were performed at day 8 and 12. We observed an increase in the level of MAG and MBP compared to negative control as a result of FGFR1 blocking, but it was not statistically significant (Figure 5.15 and Figure 5.16). It is known that FGFR1 is the high affinity receptor for both FGF1 and FGF2, and FGF2 was known to be a negative regulator of remyelination [67]. In our studies, the expression of FGF2 was shown not to be completely downregulated, but continue at a lower level until day 21 (Figure 5.10), which means that FGF2 was still present at the time points in which we performed the blocking antibody injection. Therefore, FGFR1 blocking could affect remyelination via FGF1, or FGF2, or both of them. If FGF1 exerts its effect through FGFR1, a decrease in remyelination would then occur when it was blocked. If FGFR1 is involved in remyelination process together with FGF1 and FGF2, the FGF1 effect can be expected to be neutralized and we do not expect an effect on remyelination. Observation of an increase in MAG and MBP levels upon FGFR1 blockage in this study, may indicate that FGFR1 is involved in remyelination process through FGF2 signaling since FGF2 has a negative effect on remyelination which could be removed upon FGFR1 blockage. Thus, remyelination would start earlier as observed in our study. These findings suggest that FGFR1 can have a role during remyelination process via binding to FGF2, but not to FGF1. Since the increase in myelination was not statistically significant, we may conclude that FGF2 do not inhibit remyelination alone, but together with some other molecules. These findings are in accordance with a study performed in CNS in which it has been shown that mice with genetic reduction of FGF2 or FGFR1 exhibit dramatically improved remyelination following experimental demyelination with cuprizone [68]. Apart from this possible explanation, there is still the possibility that the concentration of anti-FGFR1 neutralizing antibody used in this study was inadequate to block FGFR1

completely. Thus, further investigations should be performed to unravel FGFR1 effect during remyelination of PNS.

Since we observed a change in the level of myelin proteins as a consequence of FGFR1 blocking, we decided to investigate the pathways through which FGFR1 acts during this process. Thus, the expression of downstream signaling molecules, AKT, ERK ½ and PLC gamma 1 (Figure 5.17) were analyzed upon FGFR1 inhibition. FGFR1 autophosphorylation internally activates ERK and AKT pathways. We expected to see a decrease in phosphorylation of these proteins due to FGFR blocking, however, we could not observe a change in the levels of p-AKT and p-PLC gamma 1. The level of p-ERK ½ increased but it was again not statistically significant as the increase in MAG and MBP. According to these results, it can be suggested that the increase in the expression of MAG and MBP could be because of the increase in p-ERK ½ expression. Therefore, it can be concluded that p-ERK ½ may be involved in remyelination of Schwann cells by directly regulating the expression of myelin specific proteins.

Recently, ERK1/2 signaling was demonstrated to act in the regulation of myelin sheath thickness independent of oligodendrocyte differentiation and initiation of myelination [56, 69]. Furthermore, it has been shown that deletion of ERK1/2 in Schwann cell precursors disrupts Schwann cell differentiation and causes hypomyelination of axons, suggesting the importance of ERK1/2 signaling for PNS myelination [70]. Thus, ERK ½ can also have a role in remyelination of PNS, but it needs further investigations.

In contrast to FGFR1, blocking of FGFR2 and FGFR3 during remyelination of mouse sciatic nerve had no obvious effect on remyelination (Figure 5.19, Figure 5.20, Figure 5.21 and Figure 5.22). Thus, neither FGF1 nor FGF2 act through FGFR2 and/or FGFR3 during the remyelination of peripheral nervous system. To provide further evidence, the experiments should be repeated with higher concentrations of the blocking antibodies.

Our experiments have demonstrated that FGF1 may not act through FGF receptors, suggesting a receptor independent action in Schwann cell remyelination process. In order to further examine this possibility we also performed immunoprecipitation assays after FGF1 blocking. FGFR1, FGFR2 and FGFR3 were precipitated separately and their p-FGFR

expression were analyzed. As we expected there were no differences in p-FGFR expression in FGF1 blocked sciatic nerves compared to negative controls (Figure 5.23). This experiment further demonstrated that FGF1 may be involved in PNS remyelination in a receptor independent manner.

Apart from paracrine and autocrine pathways involving FGF receptors, FGF1 can also act through an intracrine pathway with the help of its nuclear localization signal that allows its translocation to nucleus. Recent studies have indicated that deletion of its nuclear localization signal in neural cells inhibits both its nuclear translocation and neurotrophic activity, including differentiation and cell survival. Thus, FGF1 may induce neural differentiation and protect cells from apoptosis directly *via* a nuclear pathway [41].

In a study, FGF1 was shown to be a promoter of remyelination in multiple sclerosis (MS) lesions. Transcript profiling of different types of MS lesions demonstrated that FGF1 was the most abundant of all analyzed myelin-regulating factors in remyelinated MS lesions compared to demyelinated ones. It was suggested that modulation of FGF family might improve myelin repair in MS [51]. Our findings in accordance with this study performed in CNS. Therefore, our study suggests the possibility that FGF1 may be used as a therapeutic agent for neuropathies both in PNS and CNS.

Together with studies performed previously in our laboratory, in vivo studies has further demonstrated that FGF1 has a possible role during remyelination, but probably in an intracrine manner. This study made a contribution to the knowledge about the molecular mechanism of PNS myelination that is important to unravel the pathology of peripheral neuropathies.

7. CONCLUSION

In this study, according to the previous experiments performed in our laboratory, we initially hypothesized that axonal FGF1 acts through FGF receptors that are localized to Schwann cells and involves in myelination process. Our findings provide further evidence for the involvement of FGF1 in peripheral nervous system myelination, but unlike to our hypothesis, in a receptor independent manner. Since FGF1 has a nuclear localization signal sequence, it can be suggested that FGF1 may act through its translocation into nucleus *via* its nuclear localization signal and, by this way, may regulate the expression of proteins mediating myelination process. To unravel the way through which FGF1 exerts its effect in myelination process, as a future experiment, the localization of FGF1 during remyelination period can be examined by immunohistochemical analysis, it is expressed in Schwann cells or neurons. Furthermore, generation of FGF1 conditional knock-out mice can be rewarding for further investigation of FGF1 during peripheral nervous system myelination.

According to our knowledge from the literature, this study has shown for the first time the involvement of FGF1 in peripheral nervous system myelination *via* in *vivo* experiments. Thus, it contributes to the understanding of the molecular mechanism of myelination process that is key to unravel the pathology of peripheral neuropathies and improve efficient therapeutic agents.

REFERENCES

1. Scherer, S. S., and E. J. Arroyo, "Schwann Cells", *Encyclopedia of Life Sciences*, Vol. 5, No. 1, pp. 1-9, 2005.

2. Corfas, G., M. O. Velardez, C. Ko, N. Ratner, and E. Peles, "Mechanism and Roles of Axon-Schwann Cell Interaction", *The Journal of Neuroscience*, Vol. 24, No. 42, pp. 9250-9260, 2004.

3. Maier, M., P. Berger, and U. Suter, "Understanding Schwann Cell-Neuron Interactions: the Key to Charcot-Marie-Tooth Disease?", *Journal of Anatomy*, Vol. 200, No. 4, pp. 357-366, 2000.

4. Quarles, R. H., "Myelin Sheaths: Glycoproteins Involved in Their Formation, Maintenance and Degeneration", *Cellular and Molecular Life Sciences,* Vol. 59, No. 11, pp. 1851-1871, 2002.

5. Garbay, B., A. M. Heape, F. Sargueil, and C. Cassagne, "Myelin Synthesis in the Peripheral Nervous System", *Progress in Neurobiology,* Vol. 61, No. 3, pp. 267-304, 2000.

6. Quarles, R. H., W. B. Macklin, and P. Morell, Myelin Formation, Structure and Biochemistry. In Spiegel, G., R. W. Albers, S. Brady, and D. Price (7th edition), *Basic Neurochemistry: Molecular, Cellular and Medical Aspects,* pp. 51-71, London, UK: Elseiver Academic Press, 2006.

7. Eichberg, J., "Myelin P0: New Knowledge and New Roles", *Neurochemical Research,* Vol. 27, No. 11, pp. 1331-1340, 2002.

8. Konde, V., and J. Eichberg, "Myelin Protein Zero: Mutations in the Cytoplasmic Domain Interfere With its Cellular Trafficking", *Journal of Neuroscience Research,* Vol. 83, No. 6, pp. 957-964, 2006.

9. DiVicenzo, C., C. D. Elzinga, A. C. Medeiros, I. Karbussi, J. R. Jones, M. C. Evans, C. D. Braastad, C. M. Bishop, M. Jaremko, Z. Wang, K. Liaquat, C. A. Hoffman, M. D. York, S. D. Batish, J. R. Lupski, and J. J. Higgins, "The Allelic Spectrum of Charcot-Marie-Tooth Disease in Over 17,000 Individuals with Neuropahy", *Molecular Genetics and Genomic Medicine,* Vol. 2, No. 6, pp. 522-529, 2014.

10. Snipes, G. J., and U. Suter, "Molecular Anatomy and Genetics of Myelin Proteins in the Peripheral Nervous System" *Journal of Anatomy,* Vol. 186, No. 3, pp. 483-494, 1995.

11. Li, J., B. Parker, C. Martyn, C. Natarajan, and J. Guo, "The PMP22 Gene and Its Related Diseases", *Molecular Neurobiology,* Vol. 47, No. 2, pp. 673-698, 2013.

12. Quarles, R. H., "Myelin-Associated Glycoprotein (MAG): Past, Present and Beyond", *Journal of Neurochemistry*, Vol. 100, No. 6, pp. 1431-1448, 2007.

13. Quarles, R. H., "A Hypothesis About the Relationship of Myelin-Associated Glycoprotein's Function in Myelinated Axons to its Capacity to Inhibit Neurite Outgrowth", *Neurochemistry Research*, Vol. 34, No. 1, pp. 79-86, 2009,

14. Kursula, P., "Structural Properties of Proteins Specific to the Myelin Sheath", *Amino Acids*, Vol. 34, No. 2, pp. 175-185, 2008.

15. Jessen, K. R., "Glial Cells", *The International Journal of Biochemistry and Cell Biology*, Vol. 36, No. 10, pp. 1861-1867, 2004.

16. Bhatheja., K., and J. Field, "Schwann Cells: Origin and Role in Axonal Maintenance and Regeneration", *The International Journal of Biochemistry and Cell Biology,* Vol.38, No.12, pp. 1995-1999, 2006.

17. Woodhoo, A., and Sommer, 2008, "Development of the Schwann Cell Lineage: From Neural Crest to the Myelinated Nerve", *Glia*, Vol. 56, No. 14, pp. 1481-1490, 2008.

18. Jessen, K. R., and R. Mirsky, “The Origin and Development of Glial Cells in Peripheral Nerves”, *Nature Reviews Neuroscience*, Vol. 6, No. 9, pp. 671-682, 2005.

19. Heinen, A., H. C. Lehmann, and P. Küry, “Negative Regulators of Schwann Cell Differentiation-Novel Targets for Peripheral Nerve Therapies”, *Journal of Clinical Immunology*, Vol. 33, No. 1, pp. 18-26, 2013.

20. Chan, J. R., “Myelination: All About Rac ‘n’ Roll”, *Journal of Cell Biology,* Vol. 177, No. 6, pp. 953-955, 2007.

21. Feltri, M. L., Y. Poitelon, and S. C. Previtali, “How Schwann Cells Sort Axons: New Concepts”, *The Neuroscientist*, Vol. 1, No. 1, pp. 1-14, 2015.

22. Nave, K. A. and J. L. Salzer, “Axonal Regulation of Myelination by Neurogulin 1”, *Current Opinion in Neurobioloy,* Vol. 16, No. 5, pp. 492-500, 2006.

23. Taveggia, C., G. Zanazzi, A. Petrylak, H. Yano, J. Rosenbluth, S. Einheber, X. Xu, R. M. Esper, J. A. Loeb, P. Shrager, M. V. Chao, D. L. Falls, L. Role, and J. L. Salzer, “Neurogulin 1 Type III Determines the Ensheatment Fate of Axons”, *Neuron,* Vol. 47, No. 5, pp. 681-694, 2005.

24. Newbern, J., and C. Birchmeier, “Nrg1/ErbB Signaling Networks in Schwann Cell Development and Myelination”, *Seminars in Cell and Developmental Biology,* Vol. 21, No. 9, pp. 922-928, 2010.

25. Maurel, P., S. Einheber, J. Galinsko, P. Thaker, I. Lam, M. B. Rubin, S. S. Schrere, Y. Murakami, D. H. Gutmann, and J. L. Salzer, ”Nectin-like Proteins Mediate Axon-Schwann Cell Interactions Along the Internode and Are Essential for Myelination”, *The Journal of Cell Biology,* Vol. 178, No. 5, pp. 861-874, 2007.

26. Murphy, P., P. Topilko, S. S. Maunoury, T. Seitanidou, A. B. Evercooren, and P. Charnay, “The Regulation of Krox-20 Expression Reveals Important Steps in the

Control of Peripheral Glial Cell Development", *Development,* Vol. 122*,* No. 9, pp. 2847-2857, 1996.

27. Bremer, M., F. Fröb, T. Kichko, P. Reeh, E. R. Tamm, U. Suter, and M. Wegner, "Sox-10 is Required for Schwann Cell Homeostasis and Myelin Maintenance in the Adult Peripheral Nerve, *Glia,* Vol. 59, No. 1, pp. 1022-1032, 2011.

28. Allodi, I., E. Udina, and X. Navarro, "Specificity of Peripheral Nerve Regeneration: Interactions at the Axon Level, *Progress in Neurobiology,* Vol. *98,* No. 1, pp. 16-37, 2012.

29. Kim, H. A., T. Mindos, and D. B. Parkinson, "Plastic Fantastic: Schwann Cells and Repair of the Peripheral Nervous System", *Stems Cells Translational Medicine,* Vol. 2, No. 8, pp. 553-557, 2013.

30. Papastefanaki, F., and R. Matsas, "From Demyelination to Remyelination: the Road Toward Therapies for Spinal Cord Injuries, *Glia,* Vol. 63, No. 7, pp. 1101-1125, 2015.

31. Bosse, F., "Extrinsic Cellular and Molecular Mediators of Peripheral Axonal Regeneration", *Cell and Tissue Research,* Vol. 349, No. 1, pp. 5-14, 2012.

32. Sveningsen, A. F., and L. B. Dahlin, "Repair of the Peripheral Nerve-Remyelination that Works", *Brain Sciences,* Vol. *3*, No. 3, pp. 1182-1197, 2013.

33. Arthur-Farraj, P. J., M. Latouche, D. K. Willion, S. Quintes, E. Chabrol, A. Banerjee, A. Woodhoo, B. Jenkins, M. Rahmann, M. Turmaine, G. K. Wicher, R. Mitter, L. Greensmith, A. Behrens, G. Raivich, R. Mirsky, and K. R. Jessen, "c-Jun Reprograms Schwann Cells of Injured Nerves to Generate a Repair Cell Essential for Regeneration", *Neuron,* Vol. *75,* No. 4, pp. 633-647, 2012.

34. Hall, S. M., and N. A. Gregson, "The *in vivo* and Ultrastructural Effects of Injection of Lysophosphatidyl Choline into Myelinated Peripheral Nerve Fibers of the Adult Mouse", *Journal of Cell Science,* Vol. 9, No. 3, pp. 769-789, 1971.

35. Miller, R. H., S. Fyffe-Maricich, and A. V. Caprariella, Animal Models for the Study of Multiple Scleorosis. In Con, P. M. (1st edition), *Animal Models for the Study of Human Disease,* pp. 1035-1059, London, UK: Academic Press, 2013.

36. Mason, I., "Initiation to End Point: the Multiple Roles of Fibroblast Growth Factors in Neural Development", *Nature Review Neuroscience,* Vol. 8, No. 8, pp. 583-596, 2007.

37. Itoh, N., and D. M. Ornitz, "Evolution of the *fgf* and *fgfr* Gene Families", *Trends in Genetics*, Vol. 20, No. 11, pp. 563-569, 2004.

38. Reuss, B., and O. von Bohlen und Halbach, "Fibroblast Growth Factors and Their Receptors in the Central Nervous System", *Cell and Tissue Research*, Vol. 313, No. 2, pp. 139-157, 2003.

39. Powers, C. J., McLeskey, S. W. and Wellstein, A., "Fibroblast Growth Factors, Their Receptors and Signaling", *Endocrine related cancer*, Vol. 7, No. 3, pp. 165-197, 2000.

40. Ornitz, D. M., and N. Itoh, "Fibroblast Growth Factors", *Genome Biology*, Vol. 2, No. 3, pp. 1-12, 2001,

41. Rodriquez-Enfedaque, A., S. Bouleau, M. Laurent, Y. Courtois, B. Mignotte, J. L. Vaysierre, and F. Renaud, "FGF1 Nuclear Translocation is Required for Both Its Neurotrophic Activity and Its p53-dependent Apoptosis Protection", *Biochimica et Biophysica Acta,* Vol. 1973, No. 11, pp. 1719-1727, 2009.

42. Eswarakumar, V. P., I. Lax, and J. Schlessinger, "Cellular Signaling by Fibroblast Growth Factor receptors", *Cytokine Growth Factor Review,* Vol. 16, No. 2, pp. 139-149, 2005.

43. Cruz, C. D., and F. Cruz, "The Erk 1 and 2 Pathway in the Nervous System: From Basic Aspects to Possible Clinical Applications in Pain and Visceral Dysfunction", *Current Neuropahrmocology,* Vol. 5, No. 4, pp. 244-252, 2007.

44. Papakonstanti, E. A., D. S. Emmanouel, A. Gravanis, and C. Stournaras, "Na+/Pi Co-Transport Alters Rapidly Cytoskeletal Protein Polymerization Dynamics in Opossum Kidney Cells", *Biochemistry Journal,* Vol. 315, No. 1, pp. 241-247, 1996.

45. Lanner, F., and J. Rossant, "The Role of FGF/ERK Signaling in Pluripotent Cells", *Development,* Vol. 137, No. 20, pp. 3351-3360, 2010.

46. Ford-Perris, M., H. Abud, and M. Murphy, "Fibroblast Growth Factors in the Developing Central Nervous System", *Clinical and Experimental Pharmacology and Physiology,* Vol. 28, No. 7, pp. 493-503, 2002.

47. Tagashira, S., K. Ozaki, M. Ohta, and N. Itoh, "Localization of Fibroblast Growth Factor-9 mRNA in the Rat Brain", *Molecular Brain Research,* Vol. 30, No. 2, pp. 233-241, 1995.

48. Yazaki, N., Y. Hossoi, K. Kawabata, A. Miyake, M. Minami, M. Satoh, M. Ohta, T. Kawasaki, and N. Itoh, "Differential Expression Patterns of mRNAs for Members of the Fibroblast Growth Factor Receptor Family, FGFR-1-FGFR4, in Rat Brain", *Journal of Neuroscience Research,* Vol. 37, No. 4, pp. 445-452, 1994.

49. Miyake, A., Y. Hattori, M. Ohta, and N. Itoh, "Rat Oligodendrocytes and Astrocytes Preferentially Express Fibroblast Growth Factor Receptor-2 and -3 mRNAs", *Journal of Neuroscience Research,* Vol. 45, No. 5, pp. 534-541, 1996.

50. Engele, J., and M. C. Bohn, "Effects of Acidic and Basic Fibroblast Growth Factors (aFGF, bFGF) on Glial Precursor Cell Proliferation: Age Dependency and Brain Region Specificity", *Developmental Biology,* Vol. 152, No. 2, pp. 363-372, 1992.

51. Mohan, M., A. Friese, S. Albrecht, M. Krumbholz, C. L. Elliott, A. Arthur, R. Menon, C. Farina, A. Tunker, C., Stadelmann, S. C. Barnett, I. Huitinga, H. Wekerle, R. Hohlfeld, H. Lassmann, T. Kuhlmann, C. Linington, and E. Meinl, "Transcript Profiling of Different Types of Multiple Scleorosis Lesions Yields FGF1 as a Promoter of

Remyelination", *Acta Neuropathologica Communications,* Vol. 2, No. 168, pp. 1-18, 2014.

52. Grothe, C., K. Haastert, and J. Jungnickel, "Physiological Function and Putative Therapeutic Impact of the FGF-2 System in Peripheral Nerve Regeneration-Lesions From *in vivo* Studies in Mice and Rats", *Brain Research Reviews,* Vol. 51, No. 2, pp. 293-299, 2006.

53. Jungnickel, J., A. Klutzry, S. Guhr, K. Meyer, and C. Grothe, "Regulation of Neural Death and Calcitonin Gene-Related Peptide by Fibroblast Growth Factor-2 and FGFR3 After Peripheral Nerve Injury: Evidence From Mouse Mutants", *Neuroscience,* Vol. 134, No. 4, pp. 1343-1350, 2005.

54. Lindner, M., K. Thümmler, A. Arthur, S. Brunner, C. Elliot, P. McElroy, H. Mohan, A. Williamms, J. M. Edgar, C. Schuh, C. Stadelmann, S. C. Barnett, M. Lasmann, S. Mücklisch, M. Mudaliar, N. Schaeren-Wiemers, and C. Linington, "Fibroblast Growth Factor Signaling in Multiple Scleorosis: Inhibiton of Myelination and Induction of Proinflammatory Environment by FGF9", *Brain,* Vol. 138, No. 7, pp. 1875-1893, 2015.

55. Furusho, M., J. L. Dupree, M. Bryant, and R. Bansal, "Disruption of Fibroblast Growth Factor Receptor Signaling in Nonmyelinating Schwann cells Causes Sensory Axonal Neuropathy and Impairment of Thermal Pain Sensitivity", *Journal of Neuroscience,* Vol. 29, No. 6, pp. 1608-1614, 2009.

56. Furusho, M., J. L. Dupree, K. A. Nave, and R. Bansal, "Fibroblast Growth Factor Receptor Signaling in Oligodendrocytes Regulated Myelin Sheath Thickness", *Journal of Neuroscience,* Vol. 32, No. 19, pp. 6631-6641, 2012.

57. Berger, P., A. Niemann, and U. Suter, "Schwann Cells and the Pathogenesis of Inherited Motor and Sensory Neuropathies (Charcot-Marie-Tooth Disease)", *Glia,* Vol. 54, No. 4, pp. 243-257, 2006.

58. Shy, M. E., Biology of Inherited Peripheral Neuropathies: Schwann Cell Axonal Interactions. In Espinós, C., V. Felipo, and F. Palau, *Inherited Neuromuscular Diseases,* pp. 171-181, Netharlands: Springer, 2009.

59. Perlin, J. R., M. E. Lush, W. Z. Stephens, T. Piotrowski, and W. S. Talbot, "Neural Neurogulin 1 type III Directs Schwann Cell Migration", *Development,* Vol. 138, No. 21, pp. 4639-4648, 2011.

60. Garratt, A. N., S. Britsch, and C. Birchmeier, "Neurogulin, a Factor With Many Functions in the Life of a Schwann Cell", *Bioessays,* Vol. 22, No. 11, pp. 987-996, 2000.

61. Michialov G. V., M. W. Sereda, B. G. Brinkmann, T. M. Fischer, B. Haug, C. Birchmeier, L. Role, C. Lai, M. H. Schwab, and K. A. Nave, "Axonal Neurogulin-1 Regulates Myelin Sheath Thickness", *Science*, Vol. 304, No. 5671, pp. 700-703, 2004.

62. Krishnan, A., "Neurogulin-1 Type I: a Hidden Power Within Schwann Cells for Triggering Peripheral Nerve Myelination", *Science Signaling,* Vol. 6, No. 270, 2013.

63. Spiegel, I., K. Adamsky, Y. Eshed, R. Milo, H. Sabanay, O. Sarig-Nadir, I. Harresh, S. S. Schrerer, M. N. Rasband, and E. Peles, "A Central Role for Necl4 (SynCAM4) in Schwann Cell-Axon Interaction and Myelination", *Nature Neuroscience,* Vol. 10, No. 7, pp. 861-869, 2007.

64. Dugandzija-Novaković, S., A. G. Koszowski, S. R. Levinsa, and P. Shrager, "Clustering of Na+ Channels and Node of Ranvier Formation in Remyelinating Axons", *Journal of Neuroscience,* Vol. 1, No. 2, pp. 492-503, 1995.

65. Yang, D. P., D. P. Zhang, K. S. Mak, D. E. Bonder, S. L. Pomeroy, and H. A. Kim, "Schwann Cell Proliferation During Wallerian Degeneration is not Necessary For Regeneration and Remyelination of the Peripheral Nerves: Axon-Dependent Removal of Newly Generated Schwann Cell by Apoptosis", *Molecular and Cellular Neuroscience*, Vol. 38, No.1, pp. 80-88, 2008.

66. Oberlender, S. A., and R. S. Tuan, "Application of Functional Blocking Antibodies", *Methods in Molecular Biology,* Vol. 137, No. 1, pp. 37-42, 2000.

67. Armstrong, R. C., T. Q. Le, E. E. Frost, R. C. Borke, and A. C. Vana, "Absence of Fibroblast Growth Factor 2 Promotes Oligodendroglial Repopulation of Demyelinated White Matter", *Journal of Neuroscience,* Vol. 22, No. 19, pp. 8574-8585, 2002.

68. Mierzwa, A. J., Y. X. Zhou, N. Hibbits, A. C. Vana, and R. C. Armstrong, "FGF2 and FGFR1 Signaling Regulate Functional Recovery Following Cuprizone Demyelination", *Neuroscience Letters,* Vol. 548, No. 1, pp. 280-285, 2013.

69. Ishii, A., S. L. Fyfee-Maricich, M. Furusho, R. H. Miller, and R. Bansal, "ERK1/ERK2 MAPK Signaling is Required to Increase Myelin Thickness Independent of Oligodendrocyte Differentiation and Initiation of Myelination", *The Journal of Neuroscience,* Vol. 32, No. 26, pp. 8855-8864, 2012.

70. Newbern, J. M., X. Li, S. E. Shoemaker, J. Zhou, J. Zhong, Y. Wu, D. Bonder, S. Hollenback, G. Coppola, D. H. Geschwind, G. E. Landreth, and W. B. Snider, "Specific Functions for ERK/MAPK Signaling During PNS Development", *Neuron,* Vol. 69, No. 1, pp. 91-105, 2011.